

Spin-charge separation and unconventional superconductivity in t - J model on honeycomb lattice

Jian-Jian Miao,^{1,*} Zheng-Yuan Yue,^{1,*} Hao Zhang,² Wei-Qiang Chen,^{3,4,†} and Zheng-Cheng Gu^{1,‡}

¹*Department of Physics, The Chinese University of Hong Kong, Sha Tin, New Territories, Hong Kong, China*

²*School of Physics and Astronomy, University of Minnesota, Minneapolis, MN 55455, USA*

³*Department of Physics and Shenzhen Institute for Quantum Science and Engineering, Southern University of Science and Technology, Shenzhen 518055, China*

⁴*Shenzhen Key Laboratory of Advanced Quantum Functional Materials and Devices, Southern University of Science and Technology, Shenzhen 518055, China*

(Dated: January 9, 2023)

The physical nature of doped Mott-insulator has been intensively studied for more than three decades. It is well known that the single band Hubbard model or t - J model on the bipartite lattice is the simplest model to describe a doped Mott insulator. Unfortunately, the key mechanism of superconductivity in these toy models is still under debate. In this paper, we propose a new mechanism for the $d + id$ -wave superconductivity (SC) that occurs in the small-doping region of the honeycomb lattice t - J model based on the Grassmann tensor product state numerical simulation and spin-charge separation formulation. Moreover, in the presence of anti-ferromagnetic order, a continuum effective field theory for holons is developed near half-filling. It reveals the competition between repulsive and attractive holon interactions induced by spinon fluctuations and gauge fluctuations, respectively. At a large value of t/J , the repulsive interaction dominates, leading to the non-Fermi liquid like behavior; while in a moderate range of t/J , the attractive interaction dominates, leading to the SC order. Possible experimental detection of spin-charge separation phenomena is also discussed.

I. INTRODUCTION

Since the discovery of cuprates¹, the mechanism of high- T_c superconductivity (SC) remains one of the long-standing hardcore problems in condensed matter physics. The t - J model is a well-accepted microscopic model which potentially captures the essential physics of CuO₂ layers in high- T_c cuprates, and can be derived from the large- U limit of three-band Hubbard model for the CuO₂ layers². The t - J model Hamiltonian reads:

$$H = -t \sum_{\langle ij \rangle, \sigma} (\hat{c}_{i\sigma}^\dagger \hat{c}_{j\sigma} + h.c.) + J \sum_{\langle ij \rangle} \left(\mathbf{S}_i \cdot \mathbf{S}_j - \frac{1}{4} n_i n_j \right), \quad (1)$$

where $n_i = \sum_{\sigma} c_{i\sigma}^\dagger c_{i\sigma} \equiv \sum_{\sigma} n_{i\sigma}$ is the electron density operator, $\hat{c}_{i\sigma} = (1 - n_{i,-\sigma}) c_{i\sigma}$ is the electron annihilation operator defined in no-double-occupancy subspace, and $\mathbf{S}_i = (1/2) \sum_{\alpha\beta} c_{i\alpha}^\dagger \boldsymbol{\sigma}_{\alpha\beta} c_{i\beta}$ is the spin-1/2 operator. The t -term permits the motion of holes while the J -term is the superexchange interaction.

Even though having been studied for decades, the global phase diagram of the t - J model on a square lattice is still controversial. Recently, the study of the t - J model on a honeycomb lattice attracts a lot of interest since these two types of lattices share similar features – both of them are bipartite lattices that stabilize the anti-ferromagnetic (AFM) order at half-filling. Remarkably, Grassmann tensor product state methods discovered the emergence of uniform $d + id$ -wave SC order at very small doping, while the stripe and the d -wave SC orders coexist at relatively large doping in the honeycomb lattice t - J model^{3,4}. In the weak coupling limit, the uniform $d + id$ superconductivity may also occur in the doped graphene systems revealed by various numerical methods, such as renormalized mean-field theory⁵, quantum Monte Carlo^{6–10}, renormalization group^{10–12}, and dynamical cluster approximation¹³. Other pairing symmetries, such as s and $p + ip$ waves, are also

discovered^{14–16}. Apparently, the phase diagram of the t - J model on a honeycomb lattice can provide deep insights into the key mechanism of high- T_c superconductivity on a square lattice, which is closely related to realistic experimental materials.

Three decades ago, P. W. Anderson proposed the resonating valence bond (RVB) picture to account for the high- T_c superconductivity¹⁷, and the corresponding spin-charge separation scenario is systematically studied in terms of slave-boson formalism for the t - J model¹⁸. Considering the AFM order as a characteristic feature in the small doping region, the slave-fermion formalism is a more appealing approach for small doping; the condensation of Schwinger bosons leads to a long-range magnetic order¹⁹. Nevertheless, previous slave-fermion studies of the square lattice t - J model suggested the spiral order at finite doping instead of the AFM order²⁰, which contradicts numerical and experimental results. However, as there are two sites per unit cell on honeycomb lattice, mean-field solutions with AFM order is still possible at finite doping. We believe that such kind of translation invariant mean-field theory might be crucial for the emergence of uniform $d + id$ -wave SC order.

In this paper, we first use the state-of-the-art Grassmann tensor product state numerical method to obtain the global phase diagram of t - J model on honeycomb lattice at finite doping. We adopt the slave-fermion mean-field approach and it gives rise to an AFM order on a honeycomb lattice that is consistent with our numerical results. At small doping, we find coexisting short-range AFM and FM correlations, and holon mobility. The mutual dependence of ferromagnetic (FM) correlation and holon mobility is also reproduced, which is consistent with the physics of the Nagaoka state in the infinite- U Hubbard model near half-filling²¹. We further employ the functional field integral formalism to derive the effective interacting holon theory. The effective holon Hamiltonian contains repulsive interaction generated by exchanging

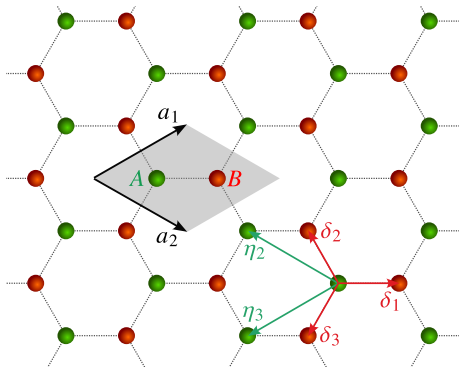


FIG. 1: The honeycomb lattice. The two triangular sub-lattices (with basis vectors $\{a_n\}_{n=1,2}$) are named A, B and colored in green, red respectively. A unit cell is shown by the shaded area. $\{\delta_n\}_{n=1,2,3}$ are nearest neighbor vectors (with $\delta_1 = a\hat{x}$, a being the nearest neighbor distance). $\{\eta_n\}_{n=1,2,3}$ are vectors to the unit cells containing the nearest neighbors, which are related to δ_n by $\eta_n = \delta_n - a\hat{x}$ (in particular $\eta_1 = 0$).

the spinons and attractive interaction via gauge fluctuations. For a moderate t/J , the attractive interaction overcomes the repulsive one and leads to the SC orders. We stress that the attractive interaction is only possible in the systems with spin-charge separation. We hope that such a mechanism can shed light on the emergence of SC orders in the t - J model on the square lattice as well and help us to understand the origin of high temperature superconductivity in cuprates.

The rest of the paper is organized as follows: Sec. II presents the Grassmann tensor product state numerical results, including the phase diagram at finite doping of the t - J model on a honeycomb lattice. The slave-fermion mean-field theory of the t - J model on honeycomb lattice is presented in Sec. III. In Sec. IV, we derive the low-energy effective interacting holon theory by including the spinon-holon coupling and gauge fluctuations. Finally, we summarize the results and discuss the potential experimental detection of spin-charge separation phenomena in Sec. V.

II. GRASSMANN TENSOR PRODUCT STATE NUMERICAL RESULTS

We first use the state-of-the-art Grassmann tensor product state method to investigate the ground state phase diagram of the t - J model on a honeycomb lattice. The ground state wave function is obtained via the so-called simple update (SU) scheme, and we also choose different bond dimensions $D = 10, 12, 14$ to examine the D dependence of the ground state energy and physical measurement such as the staggered magnetization $m = \sqrt{\langle S_i^x \rangle^2 + \langle S_i^y \rangle^2 + \langle S_i^z \rangle^2}$ (with $\langle \mathbf{S}_{i \in A} \rangle = -\langle \mathbf{S}_{i \in B} \rangle$; A, B are the two sub-lattices of the honeycomb lattice), singlet superconductivity (SC) order parameters $\Delta_s^n = \langle c_{i\uparrow} c_{i+\delta_n\downarrow} - c_{i\downarrow} c_{i+\delta_n\uparrow} \rangle / \sqrt{2}$ and triplet SC order parameters $\Delta_t^n = \langle \sum_{\alpha,\beta} c_{i\alpha} (i\sigma^y \sigma)_{\alpha\beta} c_{i+\delta_n,\beta} \rangle / \sqrt{2}$ ($\{\delta_n\}_{n=1,2,3}$ are the 3 nearest

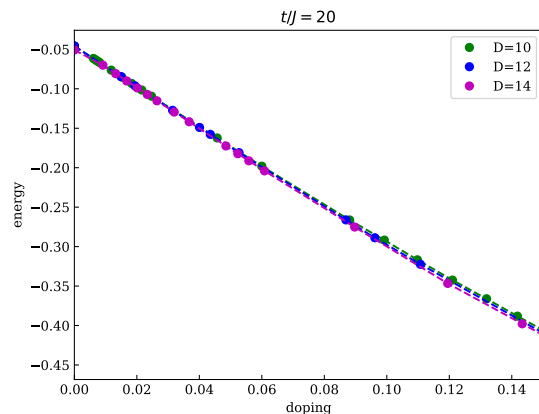


FIG. 2: Ground state energy versus doping at $t/J = 20$.

neighbor vectors of a site $i \in A$, as shown in Fig. 1).

The calculated singlet SC order parameters show $d+id$ pairing, characterized by: $\Delta_s^2/\Delta_s^1 \simeq \Delta_s^3/\Delta_s^2 \simeq \Delta_s^1/\Delta_s^3 \simeq e^{2\pi i/3}$. Similar to a previous study of $t/J = 3$ case⁴, we find the ground state energy shows very good convergence for different choices of D , e.g., for the case with $t/J = 20$ in Fig. 2. Nevertheless, very different from the $t/J = 3$ case, we find that both magnetization and SC order parameters have a rather strong D dependence, especially for larger doping. The calculated magnetization, magnitudes of singlet and triplet SC order parameters (averaged over the 3 nearest neighbors) at $t/J = 20$ are shown in Fig. 3. After proper extrapolation to the infinite D limit (see more details Appendix A), we estimate that the stagger magnetization will vanish for $\delta > 0.03$ and the singlet SC order parameter will vanish for $\delta > 0.05$. The triplet SC order parameter has a rather strong D dependence even at very small doping, and our simple extrapolation suggests it should be very close to zero at any doping.

By carefully analyzing the data at other t/J ratios, we obtain the approximate phase diagram at finite doping as shown in Fig. 4. Exactly at half-filling, the Hamiltonian of t - J model reduces to the AFM Heisenberg model. Upon doping, the AFM order is suppressed and finally vanishes, while the $d+id$ SC orders emerge. The singlet SC order dominates and exists persistently to relatively large doping (for each fixed t/J). Interestingly, for large enough t/J at each fixed doping, both AFM and SC orders eventually vanish. We conjecture that the system should enter a potentially non-Fermi liquid phase, and we shall explore the physical nature of such an exotic phase in the next two sections. The raw data determining the phase diagram are given in Appendix A.

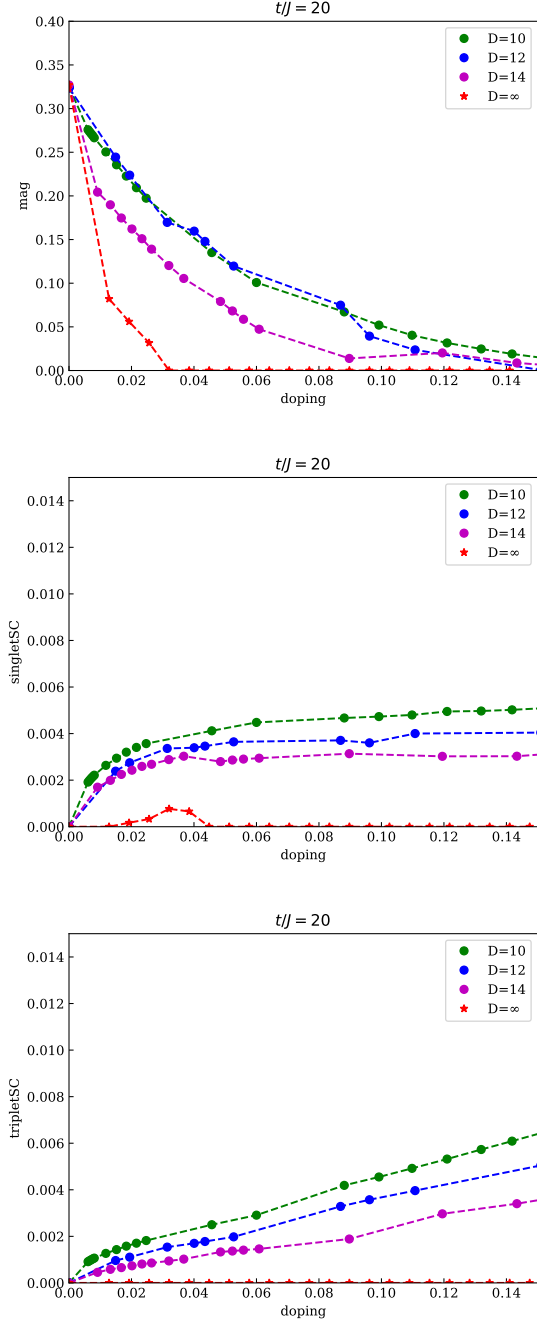


FIG. 3: Staggered magnetization, amplitudes of singlet and triplet SC order parameters versus doping at $t/J = 20$.

III. SLAVE-FERMION APPROACH

A. Mean-field theory

To gain more physical understanding for the result from numerical simulations, we first adopt the slave-fermion mean-field theory to analytically study the t - J model on the honeycomb lattice. In the slave-fermion representation, the elec-

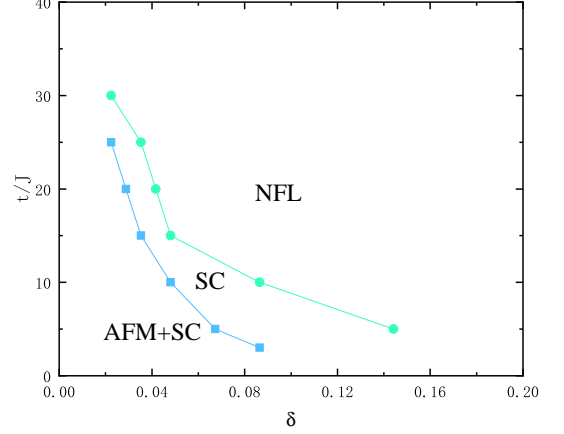


FIG. 4: The phase diagram of t - J model on honeycomb lattice at finite doping. AFM, SC, and NFL denote antiferromagnetic order, superconducting order and non-Fermi liquid phase respectively.

tron operator can be decomposed into fermionic holons and bosonic spinons in the no-double-occupancy subspace as:

$$c_{i\sigma}^\dagger = b_{i\sigma}^\dagger h_i, \quad (2)$$

where $b_{i\sigma}$ are Schwinger-boson (spinon) operators and h_i are slave-fermion (holon) operators, with no-double-occupancy constraint at each site i :

$$\sum_{\sigma} b_{i\sigma}^\dagger b_{i\sigma} + h_i^\dagger h_i = 1. \quad (3)$$

In the no-double-occupancy subspace, the spin and electron density operators on each site can be expressed in spinons only:

$$\mathbf{S}_i = \frac{1}{2} \sum_{\alpha\beta} b_{i\alpha}^\dagger \boldsymbol{\sigma}_{\alpha\beta} b_{i\beta}, \quad n_i = \hat{n}_i^b \equiv \sum_{\sigma} b_{i\sigma}^\dagger b_{i\sigma}. \quad (4)$$

Then we can re-express the t - J model Eq. (1) as:

$$H = t \sum_{\langle ij \rangle, \sigma} (h_j^\dagger h_i b_{j\sigma}^\dagger b_{i\sigma} + h.c.) - \frac{J}{2} \sum_{\langle ij \rangle} \sum_{\sigma, \sigma'} \sigma \sigma' b_{j, -\sigma}^\dagger b_{i\sigma}^\dagger b_{i\sigma'} b_{j, -\sigma'}. \quad (5)$$

Through out the whole paper, we label spin-up as $+1$, and spin-down as -1 . In the summation over bonds, we choose i to be on sub-lattice A . To obtain the mean-field theory, the no-double-occupancy constraint is only imposed *on average*:

$$\langle h_i^\dagger h_i \rangle = \delta, \quad \sum_{\sigma} \langle b_{i\sigma}^\dagger b_{i\sigma} \rangle = 1 - \delta \quad (0 \leq \delta \leq 1), \quad (6)$$

which is done by introducing chemical potentials λ_i for spinons and μ_i for holons at each site. We further define the

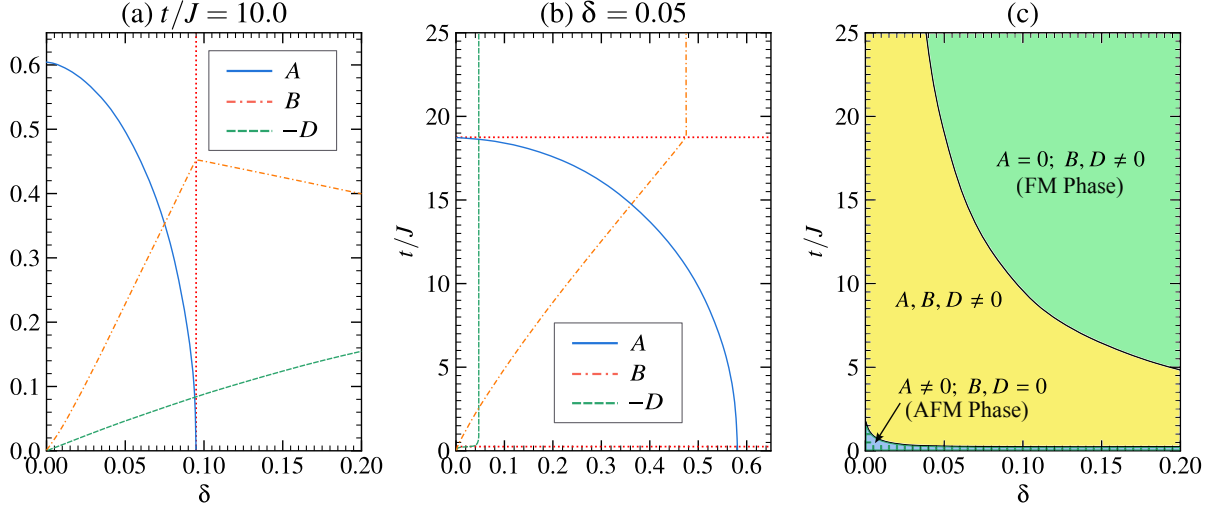


FIG. 5: Solution to the mean-field equations for doping $0 \leq \delta \leq 0.2$ on a system of 64×64 unit cells at low temperature $\beta = 800$. (a) The values of A , B and $-D$ at fixed $t/J = 10$. A second-order phase transition (indicated by a vertical dotted line) happens at $\delta = 0.09$. (b) The values of A , B and $-D$ at fixed doping $\delta = 0.05$. Phase transitions (indicated by horizontal dotted lines) happens at $t/J \approx 0.3$ (first-order) and 18.7 (second-order). (c) The mean-field phase diagram.

spinon pairing (RVB) operators and spinon hopping operators on each bond $\langle ij \rangle$ as:

$$\hat{A}_{ij} = \frac{1}{2} \sum_{\sigma} \sigma b_{i\sigma} b_{j-\sigma}, \quad \hat{B}_{ij} = \frac{1}{2} \sum_{\sigma} b_{i\sigma}^{\dagger} b_{j\sigma}. \quad (7)$$

Both are invariant under global $SU(2)$ spin rotations. The mean-field ansatz reads:

$$A_{ij} = \langle \hat{A}_{ij} \rangle, \quad B_{ij} = \langle \hat{B}_{ij} \rangle, \quad D_{ij} = \langle h_i^{\dagger} h_j \rangle. \quad (8)$$

Here $\langle \cdot \rangle$ refers to the mean-field average, and j is the nearest neighbor of i . All these parameters are in general complex numbers. We choose $i \in A$ to avoid redundancy, since $A_{ji} = -A_{ij}$, $B_{ji} = B_{ij}^*$, and $D_{ji} = D_{ij}^*$. Physically, A and B represent the short-range AFM and FM correlations respectively, and D represents the mobility of holons²⁰. In addition, we further require that:

$$\begin{aligned} \langle b_{i\sigma} b_{j\sigma'} \rangle &= \sigma A_{ij} \delta_{\sigma, -\sigma'}, \\ \langle b_{i\sigma}^{\dagger} b_{j\sigma'} \rangle &= B_{ij} \delta_{\sigma\sigma'}, \\ \langle b_{i\sigma}^{\dagger} b_{i\sigma'} \rangle &= (1/2)(1 - \delta) \delta_{\sigma\sigma'}. \end{aligned} \quad (9)$$

The mean-field Hamiltonian becomes (see details in Appendix B 1):

$$H_{\text{MF}} = H_h + H_b + H_0, \quad (10)$$

$$H_h = 2t \sum_{\langle ij \rangle} (h_i^{\dagger} h_j B_{ij}^* + h.c.) - \sum_i \mu_i h_i^{\dagger} h_i, \quad (11)$$

$$\begin{aligned} H_b &= 2t \sum_{\langle ij \rangle} (D_{ij} \hat{B}_{ij}^{\dagger} + h.c.) + \sum_{i,\sigma} \lambda_i b_{i\sigma}^{\dagger} b_{i\sigma} \\ &+ J \sum_{\langle ij \rangle} (B_{ij}^* \hat{B}_{ij} - 2A_{ij}^* \hat{A}_{ij} + h.c.), \end{aligned} \quad (12)$$

$$\begin{aligned} H_0 &= -2t \sum_{\langle ij \rangle} (D_{ij} B_{ij}^* + h.c.) - J \sum_{\langle ij \rangle} (|B_{ij}|^2 - 2|A_{ij}|^2) \\ &+ \sum_i [\mu_i \delta - \lambda_i (1 - \delta)] - \frac{3}{4} N J (1 - \delta)^2, \end{aligned} \quad (13)$$

where N is the number of *unit cells*. To keep the translation symmetry and C_3 rotation symmetry on the honeycomb lattice, we choose the *real and uniform* ansatz:

$$A_{ij} = A, \quad B_{ij} = B, \quad D_{ij} = D, \quad \mu_i = \mu, \quad \lambda_i = \lambda. \quad (14)$$

Then we perform Fourier transform

$$\begin{aligned} h_{i \in s} &= \frac{1}{\sqrt{N}} \sum_k h_k^s e^{ik \cdot R_i}, \\ b_{i \in s, \sigma} &= \frac{1}{\sqrt{N}} \sum_k b_{k\sigma}^s e^{ik \cdot R_i}. \end{aligned}$$

where $s = A, B$ labels the sub-lattice, and R_i is the position of the unit cell containing site i . Defining

$$h_k = \begin{bmatrix} h_k^A \\ h_k^B \end{bmatrix}, \quad b_{k\sigma} = \begin{bmatrix} b_{k\sigma}^A \\ b_{k\sigma}^B \end{bmatrix}, \quad (15)$$

$$r = tB, \quad p = tD + JB/2, \quad q = JA, \quad (16)$$

the mean-field Hamiltonian in momentum space is:

$$H_h = \sum_k h_k^{\dagger} H_k^h h_k, \quad (17)$$

$$H_b = \sum_k \begin{bmatrix} b_{k\uparrow}^{\dagger} & b_{-k\downarrow} \end{bmatrix} H_k^b \begin{bmatrix} b_{k\uparrow} \\ b_{-k\downarrow}^{\dagger} \end{bmatrix} - 2N\lambda, \quad (18)$$

where the Hermitian matrices H_k^h, H_k^b are defined as:

$$H_k^h = \begin{bmatrix} -\mu & \xi_k^f \\ \xi_k^{f*} & -\mu \end{bmatrix}, \quad (19)$$

$$H_k^b = \begin{bmatrix} \lambda & \xi_k^b & -\Delta_k \\ \xi_k^{b*} & \lambda & \Delta_k^* \\ -\Delta_k^* & \xi_k^b & \lambda \end{bmatrix}, \quad (20)$$

$$\xi_k^f = 2r\gamma_k, \quad \xi_k^b = p\gamma_k, \quad \Delta_k = q\gamma_k. \quad (21)$$

Here $\gamma_k = \sum_{\eta} e^{ik \cdot \eta}$ and η sums over vectors to the 3 unit cells containing nearest neighbor sites (see Fig. 1). To diagonalize Eq. (17), we define quasi-holons f_k^s (fermions) by a unitary transformation:

$$\begin{bmatrix} h_k^A \\ h_k^B \end{bmatrix} = U_k \begin{bmatrix} f_k^A \\ f_k^B \end{bmatrix}, \quad U_k \equiv \frac{1}{\sqrt{2}} \begin{bmatrix} s_r & e^{i\theta_k} \\ e^{-i\theta_k} & -s_r \end{bmatrix}, \quad (22)$$

where θ_k is the phase of γ_k (i.e. $\gamma_k = |\gamma_k|e^{i\theta_k}$), and $s_r \equiv \text{sgn}(r)$, with the definition $\text{sgn}(0) = 1$. To diagonalize Eq. (18), we define quasi-spinons $\beta_{k\sigma}^s$ (bosons) by a Bogoliubov transformation

$$\begin{bmatrix} b_{k\uparrow} \\ b_{-k\downarrow}^\dagger \end{bmatrix} = W_k \begin{bmatrix} \beta_{k\uparrow} \\ \beta_{-k\downarrow}^\dagger \end{bmatrix}, \quad (23)$$

$$W_k = \frac{1}{\sqrt{2}} \begin{bmatrix} u_k s_q e^{i\theta_k} & u_k s_q e^{i\theta_k} & v_k s_q e^{i\theta_k} & v_k s_q e^{i\theta_k} \\ u_k s_p s_q & -u_k s_p s_q & -v_k s_p s_q & v_k s_p s_q \\ -v_k s_p e^{i\theta_k} & v_k s_p e^{i\theta_k} & u_k s_p e^{i\theta_k} & -u_k s_p e^{i\theta_k} \\ v_k & v_k & u_k & u_k \end{bmatrix},$$

where $s_p = \text{sgn}(p)$, $s_q = \text{sgn}(q)$ and

$$u_k = \left(\frac{\lambda + \chi_k}{2\chi_k} \right)^{1/2}, \quad v_k = \left(\frac{\lambda - \chi_k}{2\chi_k} \right)^{1/2}, \quad (24)$$

$$\chi_k = \sqrt{\lambda^2 - |\Delta_k|^2}. \quad (25)$$

The diagonalized mean-field Hamiltonian reads:

$$H_{\text{MF}} = \sum_{k,s} E_{ks}^f f_{ks}^{s\dagger} f_k^s + \sum_{k,s,\sigma} E_{ks}^b \beta_{k\sigma}^{s\dagger} \beta_{k\sigma}^s + H_0 - 2N\lambda + \sum_{k,s} E_{ks}^b, \quad (26)$$

with quasi-holon f_k^s and quasi-spinon $\beta_{k\sigma}^s$ dispersion:

$$E_{k\pm}^f = \pm |\xi_k^f| - \mu, \quad (27)$$

$$E_{k\pm}^b = \pm |\xi_k^b| + \chi_k. \quad (28)$$

The self-consistency equations are derived by minimizing the mean-field free energy with respect to A, B, D, μ and λ :

$$\delta = \frac{1}{2N} \sum_k [n_f(E_{k+}^f) + n_f(E_{k-}^f)], \quad (29)$$

$$1 - \delta = \frac{1}{N} \sum_k \left\{ \frac{\lambda}{\chi_k} [1 + n_b(E_{k+}^b) + n_b(E_{k-}^b)] - 1 \right\}, \quad (30)$$

$$A = \frac{q}{2\alpha N} \sum_k \frac{|\gamma_k|^2}{\chi_k} [1 + n_b(E_{k+}^b) + n_b(E_{k-}^b)], \quad (31)$$

$$B = \frac{\text{sgn}(p)}{2\alpha N} \sum_k |\gamma_k| [n_b(E_{k+}^b) - n_b(E_{k-}^b)], \quad (32)$$

$$D = \frac{\text{sgn}(r)}{2\alpha N} \sum_k |\gamma_k| [n_f(E_{k+}^f) - n_f(E_{k-}^f)]. \quad (33)$$

Here $\alpha = 3$ is the coordination number; n_b and n_f are usual boson and fermion distributions defined as:

$$n_b(x) = \frac{1}{e^{\beta x} - 1}, \quad n_f(x) = \frac{1}{e^{\beta x} + 1}. \quad (34)$$

Fig. 5 shows the solution of the self-consistency equations on a honeycomb lattice of 64×64 unit cells with periodic boundary condition, calculated at $\beta = 800$, which is large enough to approximate the zero temperature behavior. Similar to previous slave-fermion mean-field theory on the square lattice^{20,22}, we obtain 3 phases in the small-doping region. When t/J is small or at zero doping, there is an AFM phase in which $A > 0$ and $B, D = 0$. As t/J increases above a certain value at finite doping, the system enters a phase with $A, B, D \neq 0$ via a first-order transition, where short-range FM and AFM correlations coexist. Note that the minimum of the spinon dispersion E_{k-}^b is always at $k = 0$; thus at zero temperature (when spinon condensation occurs), the spiral magnetic order is avoided, in contrast to the mean-field theory on the square lattice²⁰. The behavior of A, B, D in this phase is shown in Fig. 5 (a) and (b). In the upper-right part of the phase diagram there is an FM phase with $A = 0$ and $B, D \neq 0$, which is separated from the $A, B, D \neq 0$ phase by a second-order transition. This phase appears because of a large holon mobility, similar to the physics of Nagaoka states in the Hubbard model with infinite U and near half-filling. However, the FM phase is not observed from numerical simulations at large but finite t/J . We believe that the long-range FM order in this phase is an artifact of the mean-field theory, and the FM order is expected to be eliminated by gauge fluctuations induced by no-double-occupancy constraints. Below we shall discuss more details for the gauge structure for mean-field Hamiltonian.

B. Gauge structure of the mean-field Hamiltonian

Since the mean field theory does not impose the no-double-occupancy constraint on each site exactly, we must consider the gauge fluctuations to restore such a nontrivial constraint for the low energy subspace. In the slave-fermion representation Eq. (2), the physical electron operator $c_{i\sigma}$ is invariant

under the local $U(1)$ gauge transformation, i.e., for any site $i \in A, B$:

$$h_i \rightarrow h_i e^{-i\theta_i}, \quad b_{i\sigma} \rightarrow b_{i\sigma} e^{-i\theta_i}. \quad (35)$$

After projection into the no-double-occupancy physical space, each of the three phases from the mean field theory is characterized by its invariant gauge group (IGG)^{23,24}, which consists of local gauge transformations of the form Eq. (35) that leave the ansatz unchanged. The FM phase ($A = 0$ and $B, D \neq 0$) has the usual $U(1)$ gauge structure Eq. (35), with $\text{IGG} = U(1)$. However, the AFM phase ($A \neq 0$ and $B, D = 0$) has a *staggered* $U(1)$ gauge structure

$$h_{i \in s} \rightarrow h_i e^{-is\theta_i}, \quad b_{i \in s, \sigma} \rightarrow b_{i\sigma} e^{-is\theta_i}. \quad (36)$$

where we interpret $s = +1$ on sub-lattice A , and $s = -1$ on B . This opposite sign on two sub-lattices indicate opposite gauge charges on A and B sub-lattices. In the next section, we will show that such a staggered $U(1)$ gauge structure eventually leads to an effective attraction between holons on different sub-lattices, and is crucial for the emergence of superconductivity.

Finally, the $A, B, D \neq 0$ phase has a \mathbb{Z}_2 gauge structure

$$h_i \rightarrow s_i h_i, \quad b_{i\sigma} \rightarrow s_i b_{i\sigma}. \quad (37)$$

where $s_i = \pm 1$ is a sign factor depending on the site i , and the corresponding IGG is \mathbb{Z}_2 . In this phase, besides the holon and spinon quasi-particle excitations, there is another excitation corresponding to the \mathbb{Z}_2 flux of \mathbb{Z}_2 gauge fields, dubbed as vison²⁵. The \mathbb{Z}_2 gauge fluctuation corresponds to phase fluctuations of order parameters. It is coupled to the holon and spinon in a \mathbb{Z}_2 gauge invariant way and has a finite gap (if we assume the spinon does not condense), which does not confine the holon and spinon; hence it does not change the qualitative results obtained in this section. The existence of the vison excitation is an indication of fractionalization in topological order²⁶, and the corresponding topological ground state degeneracy can be detected by DMRG calculations on cylinder or torus.

IV. MECHANISM OF SUPERCONDUCTIVITY

To understand the key mechanism of SC order in the t - J model, we need to investigate the effective interactions among holons. We begin with the AFM phase with $A \neq 0$ and $B, D = 0$, and restrict the discussion to the small doping region ($\delta \ll 1$). After we establish a low energy effective field theory to understand the interactions among holons in this phase, we shall try to understand the whole phase diagram later.

A. Repulsive holon interaction at large t/J

The first step beyond the mean-field theory is to add the spinon-holon interaction from Eq. (5), and the total Hamilto-

nian reads:

$$H = H_h + H_b + H_{\text{int}}, \quad (38)$$

$$H_{\text{int}} = t \sum_{\langle ij \rangle, \sigma} (h_j^\dagger h_i b_{i\sigma}^\dagger b_{j\sigma} + h.c.). \quad (39)$$

To study the effective interaction between holons induced by the spinons, we shall use the coherent state path integral formalism. The spinon (or holon) operators are replaced by the corresponding complex (or Grassmann) numbers, with the following notations:

$$(b_{i\sigma}, b_{i\sigma}^\dagger) \rightarrow (b_{i\sigma}, \bar{b}_{i\sigma}), \quad (h_i, h_i^\dagger) \rightarrow (h_i, \bar{h}_i).$$

The partition function of fermion-boson coupled theory in the functional field integral representation is (number terms are dropped)

$$Z = \int D\bar{h} Dh D\bar{b} Db e^{-S[\bar{h}, h; \bar{b}, b]}, \quad (40)$$

$$S = S_h + S_b + S_{\text{int}}, \quad (41)$$

$$S_h = \int_0^\beta d\tau \left[\sum_i \bar{h}_i \partial_\tau h_i + H_h(\tau) \right], \quad (42)$$

$$S_b = \int_0^\beta d\tau \left[\sum_{i,\sigma} \bar{b}_{i\sigma} \partial_\tau b_{i\sigma} + H_b(\tau) \right], \quad (43)$$

$$S_{\text{int}} = \int_0^\beta d\tau H_{\text{int}}(\tau). \quad (44)$$

Now h and b are Grassmann and complex variables, denoting the holon and spinon degrees of freedom in the coherent state representation. We then integrate out spinons to derive the effective holon Hamiltonian:

$$H_h^{\text{eff}} = H_h + H_{\text{int}}^{\text{eff}}, \quad (45)$$

$$H_{\text{int}}^{\text{eff}} = \frac{1}{N} \sum_{\{k\}} V_{k_1 k_2 k'_1 k'_2} h_{k_1}^{B\dagger} h_{k_2}^{A\dagger} h_{k'_1}^A h_{k'_2}^B, \quad (46)$$

where $\sum_{\{k\}}$ is summation over all momentum with conservation ($k_1 + k_2 = k'_1 + k'_2$). In the small doping limit, $B, D \approx 0$, and the interaction strength is (see Appendix C)

$$V_{k_1 k_2 k'_1 k'_2} = -\frac{t^2}{2N} \sum_p \left\{ \frac{1}{\chi_p \chi_{p'}} (\chi_p + \chi_{p'}) \right. \\ \times \left[J_b^2 (\gamma_p^* \gamma_{p'}^* \gamma_{k'_1 - p}^* \gamma_{k_2 + p'} + \gamma_p \gamma_{p'} \gamma_{k'_1 + p}^* \gamma_{k_2 - p}) \right. \\ \left. \left. + (\chi_p \chi_{p'} - \lambda^2) (\gamma_{k'_1 + p}^* \gamma_{k_2 + p'} + \gamma_{k'_1 - p}^* \gamma_{k_2 - p}) \right] \right\}, \quad (47)$$

where $p' = p + k_1 - k'_1$, and $J_b = JA$. We have already take the static limit approximation to extract the frequency-independent effective interaction, which is mediated by exchanging two spinons with momentum p and p' . As the minimum of the spinon dispersion is at $k = 0$, the dominant contributions to the interaction coefficient in the low energy come from $p \sim p' \sim 0$, and we replace $\gamma_{k'_1 - p} \rightarrow \gamma_{k'_1}$ and $\gamma_{k_2 + p'} \rightarrow \gamma_{k_2}$

in Eq. (47), leading to

$$V_{k_1 k_2 k'_1 k'_2} \approx -t^2 \gamma_{-k'_1} \gamma_{k_2} f(k_1 - k'_1), \quad (48)$$

$$f(k) \equiv \frac{1}{N} \sum_p \frac{J_b^2 \text{Re}(\gamma_p \gamma_{p'}) + (\chi_p \chi_{p'} - \lambda^2)}{\chi_p \chi_{p'} (\chi_p + \chi_{p'})} \Big|_{p'=p+k}. \quad (49)$$

In the small doping limit, the holon momenta k_1, k'_1 are both expected to be small. Let us then calculate:

$$\begin{aligned} f(0) &= \frac{1}{N} \sum_p \frac{1}{2\chi_p^3} [J_b^2 \text{Re}(\gamma_p^2) + (\chi_p^2 - \lambda^2)] \\ &= -\frac{1}{N} \sum_p \frac{J_b^2}{\chi_p^3} (\text{Im} \gamma_p)^2 < 0, \end{aligned} \quad (50)$$

which is *negative*. Assuming a weak momentum dependence of $f(k)$, we can approximate $f(k)$ by a *negative* constant C/J_b (with $C < 0$), an inverse Fourier transform of Eq. (46) leads to a simple interaction of holons in real space:

$$\begin{aligned} H_{\text{int}}^{\text{eff}} &= -\frac{t^2 C}{J_b N} \sum_{\{k\}}' \gamma_{-k'_1} \gamma_{k_2} h_{k_1}^{B\dagger} h_{k_2}^{A\dagger} h_{k'_1}^A h_{k'_2}^B \\ &= -\frac{t^2 C}{J_b} \sum_{j \in B} \sum_{\delta, \delta'} h_j^\dagger h_{j-\delta'}^\dagger h_{j-\delta} h_j, \end{aligned} \quad (51)$$

where δ, δ' sum over the nearest neighbor vectors $\{\delta_i\}_{i=1}^3$ (see Fig. 1). In particular, $H_{\text{int}}^{\text{eff}}$ contains the following nearest-neighbor interaction terms (when $\delta = \delta'$)

$$-\frac{t^2 C}{J_b} \sum_{j \in B} \sum_{\delta} h_j^\dagger h_{j-\delta}^\dagger h_{j-\delta} h_j = -\frac{t^2 C}{J_b} \sum_{\langle ij \rangle} h_i^\dagger h_i h_j^\dagger h_j. \quad (52)$$

$C < 0$ implies that the nearest neighbor interaction between holons induced by exchanging spinons is *repulsive*.

B. $U(1)$ gauge fluctuations in the t - J Model

Next we impose the no-double-occupancy constraint on each site exactly. This is done by a delta-function in the partition function:

$$\begin{aligned} &\prod_j \delta(\bar{h}_j h_j + \sum_{\sigma} \bar{b}_{j\sigma} b_{j\sigma} - 1) \\ &= \int D\lambda \exp \left[-i \sum_j \lambda_j (\bar{h}_j h_j + \sum_{\sigma} \bar{b}_{j\sigma} b_{j\sigma} - 1) \right], \end{aligned} \quad (53)$$

where $\{\lambda_j\}$ are real Lagrange multipliers, and $D\lambda \equiv \prod_j d\lambda_j$. With the Hamiltonian Eq. (5), the coherent state path integral representation of the partition function is:

$$\begin{aligned} Z &= \int D\bar{b} D b D\bar{h} D h D\lambda e^{-\int_0^\beta d\tau L}, \\ L &= \sum_j [\bar{h}_j (\partial_\tau + i\lambda_j) h_j + \sum_{\sigma} \bar{b}_{j\sigma} (\partial_\tau + i\lambda_j) b_{j\sigma} - i\lambda_j] \\ &+ t \sum_{\langle ij \rangle, \sigma} (\bar{h}_j h_i \bar{b}_{i\sigma} b_{j\sigma} + h.c.) - \frac{J}{2} \sum_{\substack{\langle ij \rangle \\ \sigma, \sigma'}} \sigma \sigma' \bar{b}_{j-\sigma} \bar{b}_{i\sigma} b_{i\sigma'} b_{j-\sigma'}. \end{aligned}$$

The J -term is then decoupled by a Hubbard-Stratonovich transformation in the AFM channel (the FM channel is unimportant in the small-doping region). Introducing auxiliary complex fields Δ_{ij} ($i \in A, j \in B$) and their conjugate $\bar{\Delta}_{ij}$ on each bond, we arrive at

$$\begin{aligned} Z &= \int D\bar{b} D b D\bar{h} D h D\bar{\Delta} D \Delta D\lambda e^{-\int_0^\beta d\tau L}, \\ L &= \sum_j [\bar{h}_j (\partial_\tau + i\lambda_j) h_j + \sum_{\sigma} \bar{b}_{j\sigma} (\partial_\tau + i\lambda_j) b_{j\sigma}] \\ &- i \sum_j \lambda_j + t \sum_{\langle ij \rangle, \sigma} (\bar{h}_j h_i \bar{b}_{i\sigma} b_{j\sigma} + h.c.) \\ &+ \frac{J}{2} \sum_{\langle ij \rangle} [|\Delta_{ij}|^2 - \sum_{\sigma} \sigma (\bar{\Delta}_{ij} b_{i\sigma} b_{j-\sigma} + h.c.)], \end{aligned} \quad (54)$$

where $D\Delta \equiv \prod_{\langle ij \rangle} d\Delta_{ij}$ (with $i \in A$), and $|\Delta_{ij}|^2 \equiv \bar{\Delta}_{ij} \Delta_{ij}$. The Lagrangian Eq. (55) is invariant (up to a total τ -derivative term) under the staggered $U(1)$ gauge transformation:

$$\begin{aligned} b_{i \in s, \sigma} &\rightarrow b_{i\sigma} e^{-is\theta_i}, & \Delta_{ij} &\rightarrow \Delta_{ij} e^{-i(\theta_i - \theta_j)}, \\ h_{i \in s} &\rightarrow h_i e^{-is\theta_i}, & \lambda_{i \in s} &\rightarrow \lambda_i + s \partial_\tau \theta_i. \end{aligned} \quad (56)$$

The transformation can be reformulated using $U(1)$ gauge fields: define the vector potential \mathbf{A} (on bonds) and the scalar potential A_τ (on sites)

$$\theta_i - \theta_j = x_{ij} \cdot \mathbf{A}(i, j), \quad A_\tau(i) = \partial_\tau \theta_i. \quad (57)$$

Here x_{ij} is the vector from site j to site i . The gauge transformation of Δ, λ are then

$$\begin{aligned} \Delta_{ij} &\rightarrow \Delta_{ij} e^{-ix_{ij} \cdot \mathbf{A}(i, j)}, \\ \lambda_{i \in s} &\rightarrow \lambda_i + s A_\tau(i). \end{aligned} \quad (58)$$

In the partition function, we keep configurations of $\Delta_{ij}, \bar{\Delta}_{ij}, \lambda_i$ at the saddle point with fluctuations of the gauge field:

$$\begin{aligned} \Delta_{i, i+\delta} &\rightarrow \Delta e^{i\delta \cdot \mathbf{A}(i, i+\delta)} & (i \in A), \\ \bar{\Delta}_{i, i+\delta} &\rightarrow \Delta e^{-i\delta \cdot \mathbf{A}(i, i+\delta)} & (i \in A), \\ \lambda_{i \in s} &\rightarrow -i\lambda + s A_\tau(i), \end{aligned} \quad (59)$$

where $\Delta = 2A$ and λ are real solutions from the mean-field theory. The fluctuation of the norm of Δ_{ij} is ignored. Then

$$Z = \int D\bar{b} D b D\bar{h} D h D A e^{-\int_0^\beta d\tau L}, \quad (60)$$

$$L = L_h + L_{\text{heis}} + L_t + L_0, \quad (61)$$

with each part in the Lagrangian given by

$$L_h = \sum_s \sum_{i \in s} [\bar{h}_i (\partial_\tau + is A_\tau(i)) h_i + \lambda \bar{h}_i h_i], \quad (62)$$

$$\begin{aligned} L_{\text{heis}} &= \sum_s \sum_{i \in s} [\bar{b}_{i\sigma} (\partial_\tau + is A_\tau(i)) b_{i\sigma} + \lambda \bar{b}_{i\sigma} b_{i\sigma}] \\ &- \frac{J\Delta}{2} \sum_{i \in A} \sum_{\delta, \sigma} \sigma [e^{i\delta \cdot \mathbf{A}(i, i+\delta)} \bar{b}_{i\sigma} \bar{b}_{i+\delta, -\sigma} + h.c.], \end{aligned} \quad (63)$$

$$L_t = t \sum_{i \in A} \sum_{\delta, \sigma} \bar{h}_{i+\delta} h_i \bar{b}_{i\sigma} b_{i+\delta, \sigma} + h.c., \quad (64)$$

$$L_0 = - \sum_s \sum_{i \in s} (\lambda + is A_\tau(i)) + \frac{\alpha J N}{2} \Delta^2. \quad (65)$$

Here s sums over the two sub-lattices A, B . We also used the fact that the nearest neighbors of a site $i \in A$ are at positions $\{i + \delta_l\}_{l=1}^3$ on the honeycomb lattice.

We then take the continuum limit by setting the nearest neighbor distance $a \rightarrow 0$ and system size $\rightarrow \infty$. A summation over sites in one sub-lattice is replaced by an integral over space:

$$\sum_{i \in A} \text{ or } \sum_{j \in B} \rightarrow \int \frac{d^2x}{2\Omega}, \quad \Omega = \frac{3\sqrt{3}}{4}a^2. \quad (66)$$

Here a is the nearest neighbor distance, and 2Ω is the area of a unit cell. The continuum fields are

$$\begin{aligned} h_{i \in s} &\rightarrow h^s(x), & b_{i \in s, \sigma} &\rightarrow b_\sigma^s(x), \\ A_\tau(i) &\rightarrow A_\tau(x), & \mathbf{A}(i, i + \delta) &\rightarrow \mathbf{A}(x + \frac{\delta}{2}). \end{aligned} \quad (67)$$

where x is the position of the site i . For convenience, we redefine spinon-holon coupling $\alpha t \rightarrow t$, and introduce $Q \equiv \alpha J \Delta / 8$. The continuum Lagrangian is (see details in Appendix D)

$$L_h = \int \frac{d^2x}{2\Omega} \sum_s [\bar{h}^s(\partial_\tau + isA_\tau)h^s + \lambda \bar{h}^s h^s], \quad (68)$$

$$\begin{aligned} L_{\text{heis}} &= \int \frac{d^2x}{2\Omega} \sum_{s, \sigma} [\bar{b}_\sigma^s(\partial_\tau + isA_\tau)b_\sigma^s + \lambda \bar{b}_\sigma^s b_\sigma^s] \\ &+ Qa^2 \int \frac{d^2x}{2\Omega} \sum_\sigma \sigma [(\nabla - i\mathbf{A})\bar{b}_\sigma^A \cdot (\nabla + i\mathbf{A})\bar{b}_\sigma^B + h.c.] \\ &- 4Q \int \frac{d^2x}{2\Omega} \sum_\sigma \sigma [\bar{b}_\sigma^A \bar{b}_\sigma^B + h.c.], \end{aligned} \quad (69)$$

$$L_t = t \int \frac{d^2x}{2\Omega} \sum_\sigma [\bar{h}^B h^A \bar{b}_\sigma^A b_\sigma^B + h.c.], \quad (70)$$

$$L_0 = \int \frac{d^2x}{2\Omega} \left[-2\lambda + \frac{\alpha J}{2} \Delta^2 \right]. \quad (71)$$

Define $A_\mu = (A_\tau, \mathbf{A})$ and $\partial_\mu = (\partial_\tau, \nabla)$; the gauge transformation in continuum limit is

$$\begin{aligned} b_\sigma^s(x) &\rightarrow b_\sigma^s(x) e^{-is\theta(x)}, \\ h^s(x) &\rightarrow h^s(x) e^{-is\theta(x)}, \\ A_\mu(x) &\rightarrow A_\mu(x) + \partial_\mu \theta(x). \end{aligned} \quad (72)$$

C. Effective theory of holons

Following Ref. 27, we combine the Schwinger bosons into a low energy field z and a high energy field π :

$$z_\sigma = (b_\sigma^A + \sigma \bar{b}_{-\sigma}^B)/2, \quad \pi_\sigma = (b_\sigma^A - \sigma \bar{b}_{-\sigma}^B)/2. \quad (73)$$

From Eq. (72), the gauge transformation of z, π fields are

$$z_\sigma \rightarrow z_\sigma e^{-i\theta}, \quad \pi_\sigma \rightarrow \pi_\sigma e^{-i\theta}. \quad (74)$$

We then express the Lagrangian L in terms of z, π fields. The transformed L_{heis} (Eq. (69)) is

$$\begin{aligned} L_{\text{heis}} &= \int \frac{d^2x}{\Omega} \sum_\sigma \bar{z}_\sigma [(\lambda - 4Q) - Qa^2(\nabla + i\mathbf{A})^2] z_\sigma \\ &+ \int \frac{d^2x}{\Omega} \sum_\sigma [\bar{\pi}_\sigma(\partial_\tau + iA_\tau)z_\sigma - \pi_\sigma(\partial_\tau - iA_\tau)\bar{z}_\sigma] \\ &+ \int \frac{d^2x}{\Omega} \sum_\sigma \bar{\pi}_\sigma [(\lambda + 4Q) + Qa^2(\nabla + i\mathbf{A})^2] \pi_\sigma, \end{aligned} \quad (75)$$

and the spinon-holon interaction L_t (Eq. (70)) becomes

$$L_t = (-t) \int \frac{d^2x}{\Omega} \sum_\sigma \sigma (\bar{\pi}_\sigma \bar{h}^B h^A \bar{z}_{-\sigma} + h.c.). \quad (76)$$

To derive the effective theory of holons, we first integrate over the high-energy field π . The low-energy effective Lagrangian of h, z, A fields is

$$\begin{aligned} L_{hzA} &= L_0 + L_h \\ &+ \int \frac{d^2x}{\Omega} \sum_\sigma \{ (\lambda - 4Q) |z_\sigma|^2 + Qa^2 |(\nabla + i\mathbf{A})z_\sigma|^2 \\ &+ \frac{1}{\lambda + 4Q} [|(\partial_\tau + iA_\tau)z_\sigma|^2 - t^2 \bar{h}^A h^B \bar{h}^B h^A z_\sigma \bar{z}_\sigma \\ &+ t\sigma (\bar{h}^A h^B z_{-\sigma} \partial_\tau z_\sigma - \bar{h}^B h^A \bar{z}_{-\sigma} \partial_\tau \bar{z}_\sigma)] \}. \end{aligned} \quad (77)$$

After scaling $\tau \rightarrow \tau/c$ (therefore $A_\tau \rightarrow cA_\tau$) and defining

$$\begin{aligned} \Gamma &= \sqrt{\lambda^2 - 16Q^2}, & m &= \Gamma/c, \\ c &= \sqrt{Q(\lambda + 4Q)}a, & g^{-1} &= Qa^2/(c\Omega), \end{aligned} \quad (78)$$

we obtain the effective action

$$S_{hzA} = S_h + S_{zA} + S_t, \quad S_t = S_t^1 + S_t^2, \quad (79)$$

$$S_h = \frac{1}{\Omega} \int d^3x \sum_s [\bar{h}^s(\partial_\tau + isA_\tau)h^s + \frac{\lambda}{c} \bar{h}^s h^s], \quad (80)$$

$$S_{zA} = \frac{1}{g} \int d^3x \sum_\sigma [m^2 |z_\sigma|^2 + |(\partial_\mu + iA_\mu)z_\sigma|^2], \quad (81)$$

$$\begin{aligned} S_t &= \frac{t}{cg} \int d^3x \sum_\sigma \sigma (\bar{h}^A h^B z_{-\sigma} \partial_\tau z_\sigma - \bar{h}^B h^A \bar{z}_{-\sigma} \partial_\tau \bar{z}_\sigma) \\ &+ \frac{t^2}{c^2g} \int d^3x \bar{h}^A h^A \bar{h}^B h^B \sum_\sigma \bar{z}_\sigma z_\sigma. \end{aligned} \quad (82)$$

Here $\int d^3x \equiv \int_0^{c\beta} d\tau \int d^2x$, and constant terms from L_0 are dropped. Note that at half-filling, the holons are eliminated, and the effective action reduces to Eq. (81) only, which is the $\mathbb{C}P^1$ model²⁷. Let us re-express z fields as

$$\begin{aligned} z_\sigma(\tau, x) &= \sqrt{\rho_\sigma(\tau, x)} \exp[i\phi_\sigma(\tau, x)], \\ \bar{z}_\sigma(\tau, x) &= \sqrt{\rho_\sigma(\tau, x)} \exp[-i\phi_\sigma(\tau, x)]. \end{aligned} \quad (83)$$

At zero temperature, the spinon (and thus the z -field) condenses. At sufficiently low temperature, we can replace both

ρ_\uparrow and ρ_\downarrow by a number $\rho_0/2$, where ρ_0 is of the same order as the density n_0 of condensed spinons; the fluctuations of the ρ_σ fields will be ignored. Then

$$\begin{aligned} & \sum_\sigma |(\partial_\mu + iA_\mu)z_\sigma|^2 \\ &= \sum_\sigma \frac{1}{4\rho_\sigma} [(\partial_\mu \rho_\sigma)^2 + 4\rho_\sigma^2 (A_\mu + \partial_\mu \phi_\sigma)^2] \\ &\approx \sum_\sigma \rho_\sigma A_\mu^2 \approx \rho_0 A_\mu^2. \end{aligned} \quad (84)$$

In the last line, we dropped the derivative $\partial_\mu \rho_\sigma$. By a gauge transformation, the derivative of ϕ is absorbed into A_μ , and A_μ acquires a mass $\sqrt{\rho_0}$ via the Anderson-Higgs mechanism. For analysis near the mean-field saddle point, we can assume a weak τ -dependence of z and drop the τ -derivatives of z in Eq. (82). Then

$$S_{zA} \approx \frac{\rho_0}{g} \int d^3x (m^2 + A_\mu^2), \quad (85)$$

$$S_t \approx \frac{t^2 \rho_0}{c^2 g} \int d^3x \bar{h}^A h^A \bar{h}^B h^B, \quad (86)$$

yielding an effective action independent of ϕ . The integration over ϕ simply gives an (infinite) constant factor, and is dropped thereafter (this removes the gauge redundancy). We reorganize terms in S_{hzA} according to the order of A :

$$S_{hzA} = S_0 + S_1 + S_2, \quad (87)$$

$$\begin{aligned} S_0 &= S_t + \int d^3x m^2 g^{-1} \rho_0 \\ &\quad + \Omega^{-1} \int d^3x \sum_s (\bar{h}^s \partial_\tau h^s + \frac{\lambda}{c} n_s^h), \end{aligned} \quad (88)$$

$$S_1 = i\Omega^{-1} \int d^3x A_\tau (n_A^h - n_B^h), \quad (89)$$

$$S_2 = g^{-1} \int d^3x \rho_0 A_\mu^2. \quad (90)$$

Here $n_s^h \equiv \bar{h}^s h^s$ ($s = A, B$). Finally we integrate over A :

$$\begin{aligned} Z_{hzA} &\cong \int D\bar{h} Dh DA e^{-S_{hzA}} \\ &= \int D\bar{h} Dh e^{-S_0} \underbrace{\int DA e^{-(S_1+S_2)}}_{\equiv Z'} \\ Z' &\equiv \underbrace{\int DA \exp \left\{ \int d^3x (-g^{-1} \rho_0 \mathbf{A}^2) \right\}}_{\text{a constant factor}} \\ &\times \int DA_\tau \exp \left\{ \int d^3x \left[-\frac{1}{g} \rho_0 A_\tau^2 - \frac{i}{\Omega} (n_A^h - n_B^h) A_\tau \right] \right\} \\ &\propto \exp \left\{ \int d^3x \frac{g}{4\rho_0} \left[\frac{i}{\Omega} (n_A^h - n_B^h) \right]^2 \right\} \\ &= \exp \left\{ - \int d^3x \frac{g}{4\rho_0 \Omega^2} (n_A^h - n_B^h)^2 \right\}, \end{aligned}$$

Then the effective action of the holons is:

$$S_{\text{eff}} = S_0 + \int d^3x \frac{g}{4\rho_0 \Omega^2} (n_A^h - n_B^h)^2. \quad (91)$$

We identify terms representing the interaction between A -holons and B -holons (recall we redefined $\alpha t \rightarrow t$ earlier, now we restore the original t):

$$H_{\text{int}}^{AB} = \left[\frac{\alpha^2 t^2 \rho_0}{c^2 g} - \frac{g}{2\rho_0 \Omega^2} \right] \int d^2x n_A^h n_B^h. \quad (92)$$

The first term (inherited from Eq. (86)) is repulsion, produced by the exchange of two spinons between holons, in agreement with the previous calculation (in Sec. IV A) on a discrete lattice; the second term is attraction, produced by the gauge fluctuation.

The most important implication of Eq. (92) is that there exists a critical t/J below which the attraction due to gauge fluctuation should overcome the repulsion due to spinon exchange, leading to a superconducting order. For a large value of t/J , the repulsion dominates, hence the absence of SC order. This critical value of t/J is estimated from

$$\frac{\alpha^2 t^2 \rho_0}{c^2 g} \lesssim \frac{g}{2\rho_0 \Omega^2}. \quad (93)$$

Note that $\lambda \simeq 4Q$ at low temperature and small doping. Thus

$$\frac{t}{J} \lesssim \frac{\Delta}{\sqrt{2}\rho_0}. \quad (94)$$

From the mean-field calculation at half-filling and zero temperature (see Appendix B 2), we obtain $\Delta \approx 1.2$, and $\rho_0 \sim n_0 \approx 0.5$, leading to $t/J \lesssim 1.7$. However, from the renormalization group perspective (by integrating over high-energy holons)²⁸, the effective attractive between holons will renormalize to a bigger value at low energy. Thus the actual range of t/J that allows superconductivity is much larger than our naive estimation. The net attractive interaction leads to $(p + ip)$ -wave pairing of the spinless holons²⁹. Together with the singlet-pairing of the spinons, we obtain the $(d + id)$ -wave pairing of the electrons.

For the $A, B, D \neq 0$ region, the order parameter B can be regarded as an additional Higgs field which further breaks down the staggered $U(1)$ gauge field into a \mathbb{Z}_2 gauge field, and we believe that such an additional gauge field will not affect the attractive interaction in the presence of AFM long-range order. In fact, a nonzero B is also crucial for the holon mobility, e.g., for the introduction of holon kinetic term, and superconductivity is only possible in this phase. Nevertheless, at very small doping, our estimation for the effective holon interactions in previous sections is still valid since the correction induced by B is always proportional to holon concentration δ . Physically, as long as we start from the short-range RVB phase $A \neq 0$, the staggered $U(1)$ gauge fluctuations will always induce attractive interactions between holons belonging to different sub-lattices, and this naturally explains why $d + id$ SC order still survive even in the absence of AFM long-range order in this phase. We stress that the spin-charge separation

scenario plays an essential role for the emergence of SC order here, especially for the region without AFM order, and there is no other conventional picture can explain such a novel $d+id$ SC order emerged in a doped-Mott insulator!

Finally, for the region $A = 0$ and $B, D \neq 0$, the usual uniform $U(1)$ gauge fluctuations will kill the FM long-range order at finite t/J and induce repulsive interactions among holons. Such a deconfined phase of $U(1)$ gauge field does not support superconductivity and would be a natural candidate for the non-Fermi liquid phase emerged in the large t/J limit.

V. CONCLUSION AND DISCUSSION

In conclusion, we investigate the global phase diagram of the t - J model on a honeycomb lattice at small doping region using the Grassmann tensor network numerical method. Furthermore, the slave-fermion mean-field theory is employed to account for the global phase diagram. The effective interacting holon theory is rigorously derived in the presence of the AFM background. The novel phenomena of spin-charge separation and attractive interaction among holons naturally explain the emergence of $d+id$ SC orders. Remarkably, the predicted phase boundary for $d+id$ SC orders via self-consistent mean-field theory approach and effective field theory analysis is intrinsically close to the results from Grassmann tensor product numerical simulations. We stress that the spin-charge separation mechanism occurs only in strongly correlated systems and is essentially different from the weak coupling mechanism in BCS theory.

We also would like to point out that the attractive interaction between holons belonging to different sub-lattices is induced by gauge fluctuations, and the *staggered* $U(1)$ gauge structure is crucial to the attractive interaction, since in this case the two sub-lattices A and B carry opposite gauge charges. Although our derivation is in the region for $A \neq 0$ and $B, D = 0$, we believe that this mechanism is still valid in the region $A, B, D \neq 0$, and it explains the emergence of SC orders even in the absence of long-range AFM order, as long as the system is still dominated by short-range AFM spin fluctuations.

It is well known that in the conventional BCS theory, the existence of zero-energy bound fermion state in the vortex of superconductor depends on the nontrivial topological class of the bulk. According to the topological classification, the $d+id$ superconductivity discovered on the honeycomb lattice breaks the time reversal symmetry, but has the $SU(2)$ spin-rotation symmetries. Thus it belongs to the class C of ten Altland-Zirnbauer classes^{30,31}. Although the class C has no zero-energy states in the vortex from the perspective of noninteracting topological classification, we argue that the unconventional superconductivity in the t - J model on a honeycomb lattice emerges from the spin-charge separation is a different case. The bosonic spinons carrying the spin degrees of freedom condense in the AFM region. The $p+ip$ superconductivity of the spinless holons belongs to the class D and there will be a zero-energy bound state in the vortex, similar to the Majorana zero mode in conventional $p+ip$ superconductor³²⁻³⁴,

which serves as a solid evidence for the spin-charge separation scenario. Experimentally, the doped spin 1/2 honeycomb lattice antiferromagnet $\text{InV}_{1/3}\text{Cu}_{2/3}\text{O}_3$ ³⁵ would be an appealing candidate to examine the emergence of topological Majorana zero mode in its vortex core.

ACKNOWLEDGMENT

This work is supported by General Research Fund Grant No. 14302021 and NSFC/RGC Joint Research Scheme No. N-CUHK427/18 from Research Grants Council, and Direct Grant No. 4053416 from the Chinese University of Hong Kong. WQC is supported by the National Key R&D Program of China (Grants No. 2022YFA1403700), NSFC (Grants No. 11861161001), the Science, Technology and Innovation Commission of Shenzhen Municipality (No. ZDSYS20190902092905285), Guangdong Basic and Applied Basic Research Foundation under Grant No. 2020B1515120100, and Center for Computational Science and Engineering at Southern University of Science and Technology.

Appendix A: Details of the Grassmann tensor numerical calculation

We use state-of-the-art Grassmann tensor product numerical method to obtain data in Sec. II. The standard form of GTPS is used as our variational wave function. Translation-invariant ansatz is assumed and is specified by just two different Grassmann tensors \mathbf{T}_A and \mathbf{T}_B on sub-lattices A and B of each unit cell:

$$\Psi(m_i, m_j) = \text{tTr} \int \Pi_{(ij)} \mathbf{g}_{aa'} \Pi_{i \in A} \mathbf{T}_{A,abc}^{m_i} \Pi_{j \in B} \mathbf{T}_{B,a'b'c'}^{m_j}. \quad (\text{A1})$$

with

$$\begin{aligned} \mathbf{T}_{A,abc}^{m_i} &= T_{A,abc}^{m_i} \theta_\alpha^{P^f(a)} \theta_\beta^{P^f(b)} \theta_\gamma^{P^f(c)}, \\ \mathbf{T}_{B,a'b'c'}^{m_j} &= T_{B,a'b'c'}^{m_j} \theta_{\alpha'}^{P^f(a')} \theta_{\beta'}^{P^f(b')} \theta_{\gamma'}^{P^f(c')}, \\ \mathbf{g}_{aa'} &= \delta_{aa'} \mathbf{d} \theta_\alpha^{P^f(a)} \mathbf{d} \theta_{\alpha'}^{P^f(a')}. \end{aligned} \quad (\text{A2})$$

More details about this ansatz can be found in the appendix of Ref. 16. The variational ground state is obtained from the simple update imaginary time evolution algorithm³⁶. The desired doping is achieved by adjusting chemical potential. Then we measure the physical quantities by the renormalization group algorithms (GTERG/wGTERG) in Refs. 36,37. The total system size is up to 2×3^6 sites and all calculations are performed with periodic boundary conditions. We use three different virtual bond dimensions $D = 10, 12, 14$ of the GTPS. Different dopings are obtained by tuning the chemical potential.

The data of $D = \infty$ is obtained by the following approximate extrapolation method. For each fixed D , we get a series of data (δ_i^D, O_i^D) , where δ_i^D is the doping and O_i^D is the physical quantity that we are interested in. We choose some equally spaced doping points $\tilde{\delta}_i^D$. For each doping point $\tilde{\delta}_i$

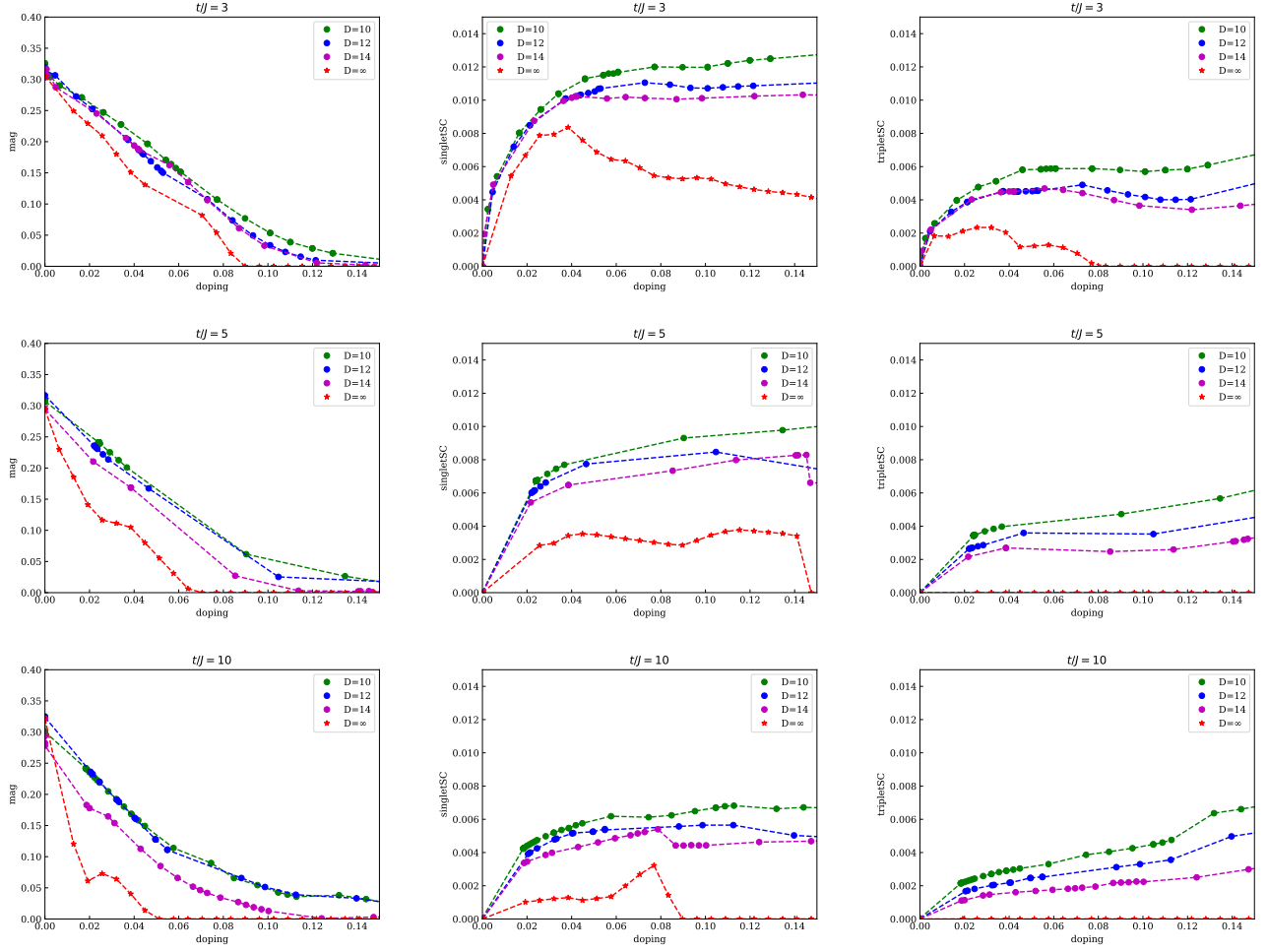


FIG. 6: Staggered magnetization, amplitudes of singlet and triplet SC order parameters versus doping at $t/J = 3, 5, 10$.

and each D , we use the linear interpolation to get the approximated \tilde{O}_i^D corresponding to $\tilde{\delta}_i$ using two nearby data points we have, $(\delta_{i,L}^D, O_{i,L}^D)$ and $(\delta_{i,R}^D, O_{i,R}^D)$,

$$\frac{\tilde{O}_i^D - O_{i,L}^D}{\tilde{\delta}_i - \delta_{i,L}^D} = \frac{O_{i,R}^D - O_{i,L}^D}{\delta_{i,R}^D - \delta_{i,L}^D}. \quad (\text{A3})$$

We then use least squares linear fit using data points (D^{-1}, \tilde{O}_i^D) and then find \tilde{O}_i^∞ by setting $D^{-1} = 0$. The linear fit $O = k_i D^{-1} + b_i$ minimizes the squared error

$$E_i = \sum_D |k_i D^{-1} + b_i - \tilde{O}_i^D|^2. \quad (\text{A4})$$

To reduce fluctuation, we use only points with good fitting (R-squared value greater than 0.7). We also set negative O_i^∞ as 0 due to physical consideration. O_i^∞ at zero doping is set to be 0 for superconducting order parameter and O_i^{14} of smallest doping we have. Here we provide figures of other values of t/J (Figs. 6, 7) below in addition to the $t/J = 20$ results in the main text (Fig. 3).

Appendix B: Details of the mean-field theory

1. Mean-field Hamiltonian of the t - J model

In this appendix, we derive the mean-field Hamiltonian Eqs. (10) to (13). The mean-field decoupling is done by ignoring higher order fluctuations around the mean-field average³⁸: for any two operators A and B ,

$$AB \approx A\langle B \rangle + \langle A \rangle B - \langle A \rangle \langle B \rangle. \quad (\text{B1})$$

The t -terms in Eq. (5) are decoupled to

$$\begin{aligned} H_t &\equiv 2t \sum_{\langle ij \rangle} (h_i^\dagger h_j \hat{B}_{ij}^\dagger + h.c.) \\ &\approx 2t \sum_{\langle ij \rangle} (D_{ij} \hat{B}_{ij}^\dagger + h_i^\dagger h_j B_{ij}^* + h.c.) \\ &\quad - 2t \sum_{\langle ij \rangle} (D_{ij} B_{ij}^* + h.c.). \end{aligned} \quad (\text{B2})$$

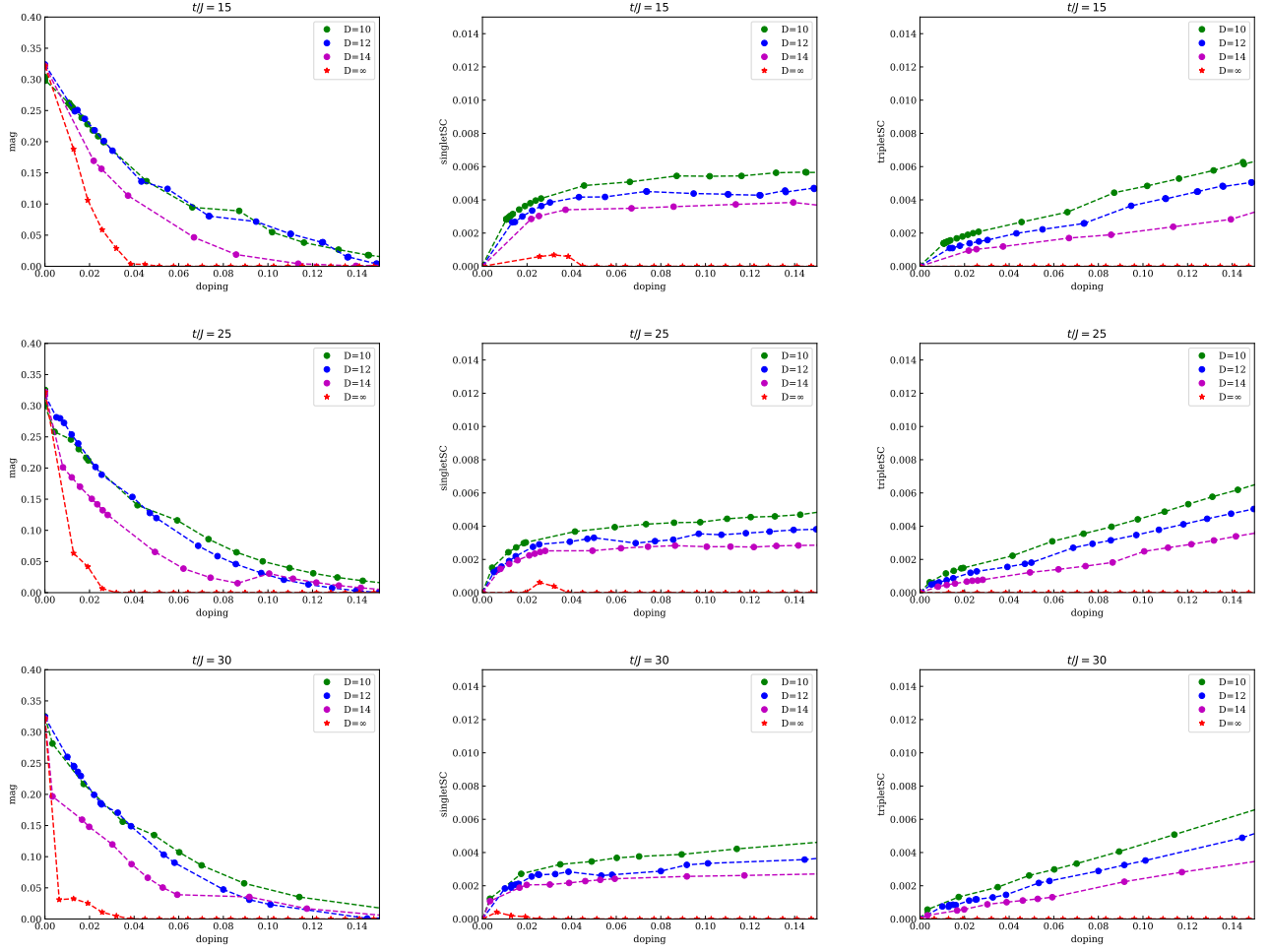


FIG. 7: Staggered magnetization, amplitudes of singlet and triplet SC order parameters versus doping at $t/J = 15, 25, 30$.

By Wick's theorem, the decoupling of J -terms in Eq. (5)

involves contribution from 3 channels:

$$H_J = -\frac{J}{2} \sum_{\langle ij \rangle} \sum_{\sigma, \sigma'} \sigma \sigma' b_{j-\sigma}^\dagger b_{i\sigma}^\dagger b_{i\sigma'} b_{j-\sigma'}$$

$$H_J \approx H_J^{(A)} + H_J^{(B)} + H_J^{(\delta)},$$

$$H_J^{(A)} = -\frac{J}{2} \sum_{\langle ij \rangle} \sum_{\sigma, \sigma'} \sigma \sigma' \left[b_{j-\sigma}^\dagger b_{i\sigma}^\dagger \langle b_{i\sigma'} b_{j-\sigma'} \rangle + \langle b_{j-\sigma}^\dagger b_{i\sigma}^\dagger \rangle b_{i\sigma'} b_{j-\sigma'} - \langle b_{j-\sigma}^\dagger b_{i\sigma}^\dagger \rangle \langle b_{i\sigma'} b_{j-\sigma'} \rangle \right],$$

$$H_J^{(B)} = -\frac{J}{2} \sum_{\langle ij \rangle} \sum_{\sigma, \sigma'} \sigma \sigma' \left[b_{j-\sigma}^\dagger b_{i\sigma'} \langle b_{i\sigma}^\dagger b_{j-\sigma'} \rangle + \langle b_{j-\sigma}^\dagger b_{i\sigma'} \rangle b_{i\sigma}^\dagger b_{j-\sigma'} - \langle b_{j-\sigma}^\dagger b_{i\sigma'} \rangle \langle b_{i\sigma}^\dagger b_{j-\sigma'} \rangle \right],$$

$$H_J^{(n)} = -\frac{J}{2} \sum_{\langle ij \rangle} \sum_{\sigma, \sigma'} \sigma \sigma' \left[b_{j-\sigma}^\dagger b_{j-\sigma'} \langle b_{i\sigma}^\dagger b_{i\sigma'} \rangle + \langle b_{j-\sigma}^\dagger b_{j-\sigma'} \rangle b_{i\sigma}^\dagger b_{i\sigma'} - \langle b_{j-\sigma}^\dagger b_{j-\sigma'} \rangle \langle b_{i\sigma}^\dagger b_{i\sigma'} \rangle \right].$$

With the mean-field ansatz Eqs. (8) and (9), we calculate the A -channel terms:

$$H_J^{(A)} = -2J \sum_{\langle ij \rangle} (A_{ij}^* \hat{A}_{ij} + h.c. - |A_{ij}|^2), \quad (\text{B3})$$

the B -channel terms:

$$\begin{aligned} H_J^{(B)} &= -\frac{J}{2} \sum_{\langle ij \rangle} \sum_{\sigma, \sigma'} \sigma \sigma' \left[B_{ij}^* b_{i\sigma}^\dagger b_{j, -\sigma'} + h.c. - |B_{ij}|^2 \right] \delta_{\sigma, -\sigma'} \\ &= \frac{J}{2} \sum_{\langle ij \rangle} \left[B_{ij}^* \sum_{\sigma} b_{i\sigma}^\dagger b_{j\sigma} + h.c. - 2|B_{ij}|^2 \right] = J \sum_{\langle ij \rangle} (B_{ij}^* \hat{B}_{ij} + h.c. - |B_{ij}|^2), \end{aligned} \quad (B4)$$

and the n -channel terms:

$$\begin{aligned} H_J^{(n)} &= -\frac{J}{2} \sum_{\langle ij \rangle} \sum_{\sigma, \sigma'} \sigma \sigma' \left[\frac{1-\delta}{2} (b_{j, -\sigma}^\dagger b_{j, -\sigma} + b_{i\sigma}^\dagger b_{i\sigma}) - \frac{(1-\delta)^2}{4} \right] \delta_{\sigma, \sigma'} \\ &= -\frac{J}{2} \sum_{\langle ij \rangle} \left[\frac{1-\delta}{2} (\hat{n}_i^b + \hat{n}_j^b) - \frac{(1-\delta)^2}{4} \right] = -\frac{1}{4} \alpha J (1-\delta) \sum_i \hat{n}_i^b + \frac{1}{4} \alpha N J (1-\delta)^2. \end{aligned} \quad (B5)$$

Here $\alpha = 3$ is the coordination number. Finally, the mean-field Hamiltonian is

$$H_{\text{MF}} = H_t + H_J + H_\delta, \quad (B6)$$

$$H_\delta = \sum_i \left[\lambda_i (\hat{n}_i^b - 1 + \delta) - \mu_i (\hat{n}_i^h - \delta) \right]. \quad (B7)$$

Here H_δ is added to impose the no-double-occupancy constraint Eq. (6), in which

$$\hat{n}_i^b = \sum_{\sigma} b_{i\sigma}^\dagger b_{i\sigma}, \quad \hat{n}_i^h = h_i^\dagger h_i.$$

Finally, we redefine λ_i by a constant shift

$$\lambda_i - \frac{1}{4} \alpha J (1-\delta) \rightarrow \lambda_i,$$

and separate H_{MF} to a holon part H_h , a spinon part H_b and a number term H_0 , leading to Eqs. (10) to (13) in the main text.

2. Spinon condensation at zero temperature

At zero temperature, Bose condensation of spinons will occur at $k = 0$, as λ decreases to the critical value λ_c determined from $\min_k E_{k-}^b = E_{0-}^b = 0$, yielding

$$\lambda_c = \sqrt{p^2 + q^2} \alpha. \quad (B8)$$

We need to modify the mean-field equations Eqs. (30) to (32) by including the density of condensed spinons at $k = 0$:

$$n_0 \equiv \frac{1}{N} \sum_{\sigma} \langle b_{0\sigma}^{s\dagger} b_{0\sigma}^s \rangle \quad (s = A, B), \quad (B9)$$

which is the same on the two sub-lattices. In the $B, D = 0$ (AFM) phase, $\lim_{\beta \rightarrow \infty} \chi_0 \rightarrow 0$, and n_0 is equal to the limit

$$n_0 = \lim_{\beta \rightarrow \infty} \frac{1}{N} \frac{\lambda}{\chi_0} [1 + 2n_b(\chi_0)]. \quad (B10)$$

In phases with $B, D \neq 0$, $\chi_0 \neq 0$. Then $n_b(E_{0-}^b)$ becomes a macroscopic number $N_0 \gg 1$, which can be related to n_0 by

$$n_0 = \frac{1}{N} \frac{\lambda}{\chi_0} (1 + N_0) \approx \frac{\lambda}{\chi_0} \frac{N_0}{N}. \quad (B11)$$

Then the modified self-consistency equations at $T = 0$ are

$$1 - \delta = n_0 + \frac{1}{N} \sum_{k \neq 0} \left[\frac{\lambda}{\chi_k} - 1 \right], \quad (B12)$$

$$A = \frac{q\alpha}{2\lambda} n_0 + \frac{q}{2\alpha N} \sum_{k \neq 0} \frac{|\gamma_k|^2}{\chi_k}, \quad (B13)$$

$$B = -\frac{p\alpha}{2\lambda} n_0 (1 - \delta_{\chi_0}), \quad (B14)$$

where $\delta_x = 1$ if $x = 0$ and 0 otherwise. In particular, at half-filling ($\delta = 0$), we get $A = 0.605$ and $n_0 = 0.484$ as $N \rightarrow \infty$. In the FM phase ($A = 0$), we get maximum condensation $n_0 = 1 - \delta$.

Appendix C: Effective holon interaction due to spinons

This appendix derives Eq. (47), the effective holon interaction by exchanging two spinons. At very small doping, we take the approximation $B, D \approx 0$. Then the spinon part of the Hamiltonian Eq. (20) is simplified to

$$H_k^b = \begin{bmatrix} \lambda & & & -\Delta_k \\ & \lambda & \Delta_k^* & \\ & \Delta_k & \lambda & \\ -\Delta_k^* & & & \lambda \end{bmatrix}, \quad (C1)$$

where $\Delta_k = J_b \gamma_k$ (with $J_b = JA$). We then Fourier transform the holons and spinons to momentum-frequency representation:

$$h_k^s(\tau) = \frac{1}{\sqrt{\beta}} \sum_{k, \omega} e^{i\omega\tau} h_{k\omega}^s, \quad (C2)$$

$$b_{k\sigma}^s(\tau) = \frac{1}{\sqrt{\beta}} \sum_{k, \nu} e^{i\nu\tau} b_{k\nu\sigma}^s, \quad (C3)$$

where ω, ν sum over discrete fermion and boson Matsubara frequencies, respectively. The spinon part of the action is

$$S_b = \sum_{k, k'} \sum_{\nu, \nu'} \left[\bar{b}_{k\nu\uparrow}, b_{-k, -\nu\downarrow} \right] (G_0)_{k\nu, k'\nu'}^{-1} \begin{bmatrix} b_{k'\nu'\uparrow} \\ \bar{b}_{-k', -\nu'\downarrow} \end{bmatrix}, \quad (C4)$$

where we introduced the shorthand notation

$$b_{kv\sigma} \equiv \begin{bmatrix} b_{kv\sigma}^A \\ b_{kv\sigma}^B \end{bmatrix},$$

and the matrix G_0 is (with $\chi_k = \sqrt{\lambda^2 - |\Delta_k|^2}$):

$$(G_0)_{kv,k'\nu'} = (\mathcal{G}_0)_{kv} \delta_{k-k'} \delta_{\nu-\nu'}, \quad (C5)$$

$$(\mathcal{G}_0)_{kv} \equiv \frac{1}{\nu^2 + \chi_k^2} \begin{bmatrix} \lambda - i\nu & & \Delta_k \\ & \lambda - i\nu & -\Delta_k^* \\ & -\Delta_k & \lambda + i\nu \\ \Delta_k^* & & \lambda + i\nu \end{bmatrix}. \quad (C6)$$

Action terms corresponding to spinon-holon interaction Eq. (39) is Fourier transformed to (with $\gamma_k = \sum_{\eta} e^{ik\cdot\eta}$):

$$S_{\text{int}} = \sum_{k,k'} \sum_{\nu',\nu''} [\bar{b}_{k\nu'\uparrow}, b_{-k,-\nu''\downarrow}] T_{k\nu',k'\nu''} \begin{bmatrix} b_{k'\nu''\uparrow} \\ \bar{b}_{-k',-\nu''\downarrow} \end{bmatrix}, \quad (C7)$$

$$T_{k\nu',k'\nu''} = \begin{bmatrix} t_1^{AB} & t_1^{BA} \\ t_2^{BA} & t_2^{AB} \end{bmatrix}_{k\nu',k'\nu''}. \quad (C8)$$

The matrix elements of T are

$$t_{1,k\nu',k'\nu''}^{AB} = \frac{t}{\beta N} \sum_q \sum_{\omega,\omega'} \bar{h}_{k'+q,\omega}^A h_{k+q,\omega'}^B \gamma_{q,\omega}, \quad (C9)$$

$$t_{2,k\nu',k'\nu''}^{AB} = \frac{t}{\beta N} \sum_q \sum_{\omega,\omega'} \bar{h}_{k'+q,\omega}^A h_{k+q,\omega'}^B \gamma_{q+k+k'}, \quad (C10)$$

$$t_{1,k\nu',k'\nu''}^{BA} = \frac{t}{\beta N} \sum_q \sum_{\omega,\omega'} \bar{h}_{k'+q,\omega}^B h_{k+q,\omega'}^A \gamma_q^*, \quad (C11)$$

$$t_{2,k\nu',k'\nu''}^{BA} = \frac{t}{\beta N} \sum_q \sum_{\omega,\omega'} \bar{h}_{k'+q,\omega}^B h_{k+q,\omega'}^A \gamma_{q+k+k'}^*, \quad (C12)$$

where

$$\sum'_{\omega,\omega'} \equiv \sum_{\omega,\omega'} \delta_{(\nu+\omega)-(\nu'+\omega')}. \quad (C13)$$

To obtain an effective theory for the holons, we integrate out the spinons. Collecting terms involving spinons in the action,

we get

$$S_b + S_{\text{int}} = \sum_{k,k'} \sum_{\nu',\nu''} [\bar{b}_{k\nu'\uparrow}, b_{-k,-\nu''\downarrow}] G_{k\nu',k'\nu''}^{-1} \begin{bmatrix} b_{k'\nu''\uparrow} \\ \bar{b}_{-k',-\nu''\downarrow} \end{bmatrix},$$

where the matrix G^{-1} is given by

$$G_{k\nu',k'\nu''}^{-1} = (G_0^{-1} + T)_{k\nu',k'\nu''}. \quad (C14)$$

The effective action for holons $S_h^{\text{eff}}[\bar{h}, h]$ is defined by

$$Z = \int D\bar{h} Dh e^{-S_h^{\text{eff}}[\bar{h}, h]},$$

$$e^{-S_h^{\text{eff}}} \equiv \int D\bar{b} Db e^{-S} = e^{-S_h} \int D\bar{b} Db e^{-(S_b + S_{\text{int}})}.$$

Performing Gaussian integration over spinons, we get

$$\int D\bar{b} Db e^{-(S_b + S_{\text{int}})} \propto (\det G^{-1})^{-1} = \exp(-\ln \det G^{-1}). \quad (C15)$$

Thus the effective holon action is given by

$$S_h^{\text{eff}} = S_h + \ln \det G^{-1}. \quad (C16)$$

The log-determinant can be expanded as a power series of t ; using $\ln \det A = \text{tr} \ln A$ and $\ln(1+x) = \sum_{n=1}^{\infty} (-1)^{n+1} x^n/n$, we obtain

$$\begin{aligned} \ln \det G^{-1} &= \text{tr} \ln(G_0^{-1} + T) \\ &= \text{tr}[\ln G_0^{-1} + \ln(1 + G_0 T)] \\ &= \text{tr} \ln G_0^{-1} + \sum_{n=1}^{\infty} \frac{(-1)^{n+1}}{n} \text{tr}(G_0 T)^n. \end{aligned} \quad (C17)$$

The term $\text{tr} \ln G_0^{-1}$ is a constant independent of h and can be omitted. Then the effective holon action is

$$S_h^{\text{eff}}[\bar{h}, h] = S_h^0 + \sum_{n=1}^{\infty} S_h^n, \quad (C18)$$

$$S_h^n \equiv \frac{(-1)^{n+1}}{n} \text{tr}(G_0 T)^n. \quad (C19)$$

We keep up to second order terms. The first order term $\text{tr}(G_0 T) = 0$. The second order term is

$$\begin{aligned} S_h^2 &\equiv -\frac{1}{2} \text{tr}(G_0 T)^2 = -\frac{1}{2} \sum_{k,\nu} \sum_{k_1\nu_1} \sum_{k_2\nu_2} \sum_{k'\nu'} \text{tr}[(G_0)_{k\nu,k_1\nu_1} T_{k_1\nu_1,k_2\nu_2} (G_0)_{k_2\nu_2,k'\nu'} T_{k'\nu',k\nu}] \\ &= \frac{1}{2} \sum_{k,\nu} \sum_{k',\nu'} \frac{1}{(\nu^2 + \chi_k^2)(\nu'^2 + \chi_{k'}^2)} \left[\Delta_k \Delta_{k'} (t_1^{AB} t_2^{BA} + t_2^{BA} t_1^{AB}) + \Delta_k^* \Delta_{k'}^* (t_1^{BA} t_2^{AB} + t_2^{AB} t_1^{BA}) \right. \\ &\quad \left. - (i\nu - \lambda)(i\nu' - \lambda)(t_1^{AB} t_1^{BA} + t_1^{BA} t_1^{AB}) - (i\nu + \lambda)(i\nu + \lambda')(t_2^{AB} t_2^{BA} + t_2^{BA} t_2^{AB}) \right]. \end{aligned}$$

Here we simply write $t_i^{s's'} = t_{i,k\nu,k'\nu'}^{s's'}$, $t_i'^{s's'} = t_{i,k'\nu',k\nu}^{s's'}$ (where $s, s' = A, B$ and $i = 1, 2$). Note that each term is invariant under the

exchange of $(k, \nu) \leftrightarrow (k', \nu')$. Then

$$S_h^2 = \sum_{k, \nu} \sum_{k', \nu'} \frac{1}{(\nu^2 + \chi_k^2)(\nu'^2 + \chi_{k'}^2)} \left[\Delta_k \Delta_{k'} t_2^{BA} t_1^{*AB} + \Delta_k^* \Delta_{k'}^* t_1^{BA} t_2^{*AB} \right. \\ \left. - (i\nu - \lambda)(i\nu' - \lambda) t_1^{BA} t_1^{*AB} - (i\nu + \lambda)(i\nu' + \lambda) t_2^{BA} t_2^{*AB} \right].$$

Evaluating summation over ν' first after substituting in the definition of $t_i^{ss'}$ (Eqs. (C9) to (C12)), we obtain:

$$S_h^2 = \left(\frac{t}{\beta N} \right)^2 \sum_{k, \nu} \sum_{k', \nu'} \sum_{q_1, q_2} \sum_{\omega_1, \omega'_1} \sum_{\omega_2, \omega'_2} \frac{\delta_{(\nu+\omega_1)-(\nu'+\omega'_1)} \delta_{(\nu'+\omega_2)-(\nu+\omega'_2)}}{(\nu^2 + \chi_k^2)(\nu'^2 + \chi_{k'}^2)} \bar{h}_{k'+q_1, \omega'_1}^B h_{k+q_1, \omega_1}^A \bar{h}_{k+q_2, \omega_2}^A h_{k'+q_2, \omega'_2}^B \\ \times \left[\Delta_k \Delta_{k'} \gamma_{q_1+k+k'}^* \gamma_{q_2} + \Delta_k^* \Delta_{k'}^* \gamma_{q_1}^* \gamma_{q_2+k+k'} - (i\nu - \lambda)(i\nu' - \lambda) \gamma_{q_1}^* \gamma_{q_2} - (i\nu + \lambda)(i\nu' + \lambda) \gamma_{q_1+k+k'}^* \gamma_{q_2+k+k'} \right] \\ = \left(\frac{t}{\beta N} \right)^2 \sum_{k, k', \nu} \sum_{q_1, q_2} \sum_{\{\omega\}} \frac{1}{(\nu^2 + \chi_k^2)[(\nu + \omega_1 - \omega'_1)^2 + \chi_{k'}^2]} \bar{h}_{k'+q_1, \omega'_1}^B h_{k+q_1, \omega_1}^A \bar{h}_{k+q_2, \omega_2}^A h_{k'+q_2, \omega'_2}^B \\ \times \left[\Delta_k \Delta_{k'} \gamma_{q_1+k+k'}^* \gamma_{q_2} + \Delta_k^* \Delta_{k'}^* \gamma_{q_1}^* \gamma_{q_2+k+k'} \right. \\ \left. - (i\nu - \lambda)[i(\nu + \omega_1 - \omega'_1) - \lambda] \gamma_{q_1}^* \gamma_{q_2} - (i\nu + \lambda)[i(\nu + \omega_1 - \omega'_1) + \lambda] \gamma_{q_1+k+k'}^* \gamma_{q_2+k+k'} \right], \quad (\text{C20})$$

where

$$\sum_{\{\omega\}}' \equiv \sum_{\omega_1, \omega'_1} \sum_{\omega_2, \omega'_2} \delta_{(\omega_1+\omega_2)-(\omega'_1+\omega'_2)}$$

We keep only the *instantaneous* holon interaction by taking the *static limit*, i.e. setting $\omega_1 = \omega'_1$ in the coefficient of $\bar{h}^B h^A \bar{h}^A h^B$. Then Eq. C20 reduces to

$$S_h^2 = \left(\frac{t}{\beta N} \right)^2 \sum_{k, k', \nu} \sum_{q_1, q_2} \sum_{\{\omega\}} \frac{\bar{h}_{k'+q_1, \omega'_1}^B h_{k+q_1, \omega_1}^A \bar{h}_{k+q_2, \omega_2}^A h_{k'+q_2, \omega'_2}^B}{(\nu^2 + \chi_k^2)(\nu^2 + \chi_{k'}^2)} \\ \times \left[\Delta_k \Delta_{k'} \gamma_{q_1+k+k'}^* \gamma_{q_2} + \Delta_k^* \Delta_{k'}^* \gamma_{q_1}^* \gamma_{q_2+k+k'} - (i\nu - \lambda)^2 \gamma_{q_1}^* \gamma_{q_2} - (i\nu + \lambda)^2 \gamma_{q_1+k+k'}^* \gamma_{q_2+k+k'} \right]. \quad (\text{C21})$$

In the zero-temperature limit, the summation over ν can be replaced by an integral:

$$\frac{1}{\beta} \sum_{\nu} \rightarrow \int \frac{d\nu}{2\pi}, \\ \int \frac{d\nu}{2\pi} \frac{1}{(\nu^2 + \chi_k^2)(\nu^2 + \chi_{k'}^2)} = \frac{1}{2\chi_k \chi_{k'} (\chi_k + \chi_{k'})}, \\ \int \frac{d\nu}{2\pi} \frac{(i\nu \pm \lambda)^2}{(\nu^2 + \chi_k^2)(\nu^2 + \chi_{k'}^2)} = \frac{\lambda^2 - \chi_k \chi_{k'}}{2\chi_k \chi_{k'} (\chi_k + \chi_{k'})}.$$

We can then inverse Fourier transform ω to τ :

$$\frac{1}{\beta} \sum_{\{\omega\}}' \bar{h}_{k'+q_1, \omega'_1}^B \bar{h}_{k+q_2, \omega_2}^A h_{k+q_1, \omega_1}^A h_{k'+q_2, \omega'_2}^B \\ = \int d\tau \bar{h}_{k'+q_1, \tau}^B \bar{h}_{k+q_2, \tau}^A h_{k+q_1, \tau}^A h_{k'+q_2, \tau}^B. \quad (\text{C22})$$

Therefore (the order of h is changed)

$$S_h^2 = -\frac{t^2}{2N^2} \sum_{k, k'} \sum_{q_1, q_2} \frac{\bar{h}_{k'+q_1}^B \bar{h}_{k+q_2}^A h_{k+q_1}^A h_{k'+q_2}^B}{\chi_k \chi_{k'} (\chi_k + \chi_{k'})} \\ \times \left[\Delta_k \Delta_{k'} \gamma_{q_1+k+k'}^* \gamma_{q_2} + \Delta_k^* \Delta_{k'}^* \gamma_{q_1}^* \gamma_{q_2+k+k'} \right. \\ \left. + (\chi_k \chi_{k'} - \lambda^2) (\gamma_{q_1}^* \gamma_{q_2} + \gamma_{q_1+k+k'}^* \gamma_{q_2+k+k'}) \right]. \quad (\text{C23})$$

Redefining summation variables:

$$\left. \begin{array}{l} k_1 = k + q_1 \\ k_2 = k' + q_2 \\ q = k' - k \\ p = -k' \end{array} \right\} \Rightarrow \left\{ \begin{array}{l} k = -p - q \\ k' = -p \\ q_1 = k_1 + p + q \\ q_2 = k_2 + p \end{array} \right.,$$

we obtain

$$S_h^2 = -\frac{t^2}{2N^2} \sum_{k_1, k_2} \sum_{p, q} \frac{\bar{h}_{k_1+q}^B \bar{h}_{k_2-q}^A h_{k_1}^A h_{k_2}^B}{\chi_{p+q} \chi_p (\chi_{p+q} + \chi_p)} \\ \times \left[\Delta_{p+q}^* \Delta_p^* \gamma_{k_1-p}^* \gamma_{k_2+p} + \Delta_{p+q} \Delta_p \gamma_{k_1+p+q}^* \gamma_{k_2-p-q} \right. \\ \left. + (\chi_{p+q} \chi_p - \lambda^2) (\gamma_{k_1+p+q}^* \gamma_{k_2+p} + \gamma_{k_1-p}^* \gamma_{k_2-p-q}) \right]. \quad (\text{C24})$$

Here we used

$$\chi_{-k} = \chi_k, \quad \gamma_{-k} = \gamma_k^*, \quad \Delta_{-k} = \Delta_k^*.$$

From this effective action, we read off terms in the Hamiltonian that represent interaction between holons (rename k_1, k_2 to k, k'):

$$\begin{aligned} H_{\text{int}}^{\text{eff}} &= \frac{1}{N} \sum_{k, k', q} V_{kk'q} h_{k+q}^{B\dagger} h_{k'-q}^{A\dagger} h_k^A h_{k'}^B, \\ V_{kk'q} &\equiv -\frac{t^2}{2N} \sum_p \frac{1}{\chi_{p+q} \chi_p (\chi_{p+q} + \chi_p)} \\ &\times \left[\Delta_{p+q}^* \Delta_p^* \gamma_{k-p}^* \gamma_{k'+p} + \Delta_{p+q} \Delta_p \gamma_{k+p+q}^* \gamma_{k'-p-q} \right. \\ &\left. + (\chi_{p+q} \chi_p - \lambda^2) (\gamma_{k+p+q}^* \gamma_{k'+p} + \gamma_{k-p}^* \gamma_{k'-p-q}) \right]. \end{aligned} \quad (\text{C25})$$

This effective holon interaction is due to the exchange of two spinons of momenta p and $p+q$. Let us call the holon momenta as

$$k+q = k_1, \quad k = k'_1, \quad k' = k'_2, \quad k'_2 + k'_1 - k_1 = k_2.$$

Then we get an alternative expression of $H_{\text{int}}^{\text{eff}}$:

$$\begin{aligned} H_{\text{int}}^{\text{eff}} &= \frac{1}{N} \sum_{\{k, k'\}} V_{k_1 k_2 k'_1 k'_2} h_{k_1}^{B\dagger} h_{k_2}^{A\dagger} h_{k'_1}^A h_{k'_2}^B, \\ V_{k_1 k_2 k'_1 k'_2} &\equiv -\frac{t^2}{2N} \sum_p \frac{\delta_{(k_1+k_2)-(k'_1+k'_2)}}{\chi_p \chi_{p+k_1-k'_1} (\chi_p + \chi_{p+k_1-k'_1})} \\ &\times \left[\Delta_p^* \Delta_{p+k_1-k'_1}^* \gamma_{k'_1-p}^* \gamma_{k_2+p} + \Delta_p \Delta_{p+k_1-k'_1} \gamma_{k_1+p}^* \gamma_{k_2-p} \right. \\ &\left. + (\chi_p \chi_{p+k_1-k'_1} - \lambda^2) (\gamma_{k_1+p}^* \gamma_{k_2+p} + \gamma_{k'_1-p}^* \gamma_{k_2-p}) \right]. \end{aligned} \quad (\text{C27})$$

Define $p' \equiv p + k_1 - k'_1$. We then rewrite the expression by keeping k'_1, k_2 (the momenta of h^A) only:

$$\begin{aligned} V_{k_1 k_2 k'_1 k'_2} &\equiv -\frac{t^2}{2N} \sum_p \left\{ \frac{\delta_{(k_1+k_2)-(k'_1+k'_2)}}{\chi_p \chi_{p'} (\chi_p + \chi_{p'})} \right. \\ &\times \left[\Delta_p^* \Delta_{p'}^* \gamma_{k'_1-p}^* \gamma_{k_2+p'} + \Delta_p \Delta_{p'} \gamma_{k'_1+p'}^* \gamma_{k_2-p} \right. \\ &\left. \left. + (\chi_p \chi_{p'} - \lambda^2) (\gamma_{k'_1+p'}^* \gamma_{k_2+p'} + \gamma_{k'_1-p}^* \gamma_{k_2-p}) \right] \right\}. \end{aligned} \quad (\text{C28})$$

Finally, with

$$\sum_{\{k\}}' \equiv \sum_{k_1, k_2} \sum_{k'_1, k'_2} \delta_{(k_1+k_2)-(k'_1+k'_2)}$$

we get (substituting in $\Delta_k = J_b \gamma_k$)

$$\begin{aligned} H_{\text{int}}^{\text{eff}} &= \frac{1}{N} \sum_{\{k\}}' V_{k_1 k_2 k'_1 k'_2} h_{k_1}^{B\dagger} h_{k_2}^{A\dagger} h_{k'_1}^A h_{k'_2}^B, \\ V_{k_1 k_2 k'_1 k'_2} &= -\frac{t^2}{2N} \sum_p \left\{ \frac{1}{\chi_p \chi_{p'} (\chi_p + \chi_{p'})} \right. \\ &\times \left[J_b^2 (\gamma_p^* \gamma_{p'}^* \gamma_{k'_1-p}^* \gamma_{k_2+p'} + \gamma_p \gamma_{p'} \gamma_{k'_1+p'}^* \gamma_{k_2-p}) \right. \\ &\left. \left. + (\chi_p \chi_{p'} - \lambda^2) (\gamma_{k'_1+p'}^* \gamma_{k_2+p'} + \gamma_{k'_1-p}^* \gamma_{k_2-p}) \right] \right\}, \end{aligned} \quad (\text{C29})$$

which is Eq. (47).

Appendix D: Continuum limit of the t - J model Lagrangian

This section derives the Lagrangian Eqs. (68) to (71) in the continuum limit. The following identities on the honeycomb lattice are useful:

$$\begin{aligned} \sum_{\delta} \delta \cdot \mathbf{A} &= 0, \\ \sum_{\delta} (\delta \cdot \nabla)^2 f &= (\alpha/2) a^2 \nabla^2 f, \\ \sum_{\delta} (\delta \cdot \mathbf{A})(\delta \cdot \mathbf{B}) &= (\alpha/2) a^2 \mathbf{A} \cdot \mathbf{B}, \\ \sum_{\delta} (\delta \cdot \mathbf{A})^2 &= (\alpha/2) a^2 \mathbf{A}^2. \end{aligned}$$

Here a is the nearest neighbor distance, δ sums over nearest neighbors of a site on sub-lattice A (see Fig. 1), f, g are any scalar fields and \mathbf{A}, \mathbf{B} are any vector fields. The continuum limit of L_h (Eq. (62)) and L_0 (Eq. (65)) are

$$L_h = \int \frac{d^2x}{2\Omega} \sum_s [\bar{h}^s (\partial_\tau + isA_\tau) h^s + \lambda \bar{h}^s h^s], \quad (\text{D1})$$

$$\begin{aligned} L_0 &= \int \frac{d^2x}{2\Omega} \left[-\sum_s (\lambda + isA_\tau) + \frac{\alpha J}{2} \Delta^2 \right] \\ &= \int \frac{d^2x}{2\Omega} \left[-2\lambda + \frac{\alpha J}{2} \Delta^2 \right]. \end{aligned} \quad (\text{D2})$$

The continuum limit of the spinon-holon interaction L_t (Eq. (64)) is

$$\begin{aligned} L_t &\rightarrow t \int \frac{d^2x}{2\Omega} \sum_{\delta, \sigma} \\ &[\bar{h}^B(x+\delta) h^A(x) \bar{b}_\sigma^A(x) b_\sigma^B(x+\delta) + h.c.] \\ &\approx t \int \frac{d^2x}{2\Omega} \sum_{\delta, \sigma} \left\{ [(1 + \delta \cdot \nabla + \frac{1}{2}(\delta \cdot \nabla)^2) \bar{h}^B] h^A \right. \\ &\left. \times \bar{b}_\sigma^A [(1 + \delta \cdot \nabla + \frac{1}{2}(\delta \cdot \nabla)^2) b_\sigma^B] + h.c. \right\}. \end{aligned}$$

We expand this in powers of the nearest neighbor distance a . The first order terms in a turn out to vanish. The second order terms are not important in describing the spinon-holon interaction. We then only keep the zeroth order terms:

$$\begin{aligned} L_t &\approx t \int \frac{d^2x}{2\Omega} \sum_{\delta, \sigma} (\bar{h}^B h^A \bar{b}_\sigma^A b_\sigma^B + h.c.) \\ &= at \int \frac{d^2x}{2\Omega} \sum_{\sigma} (\bar{h}^B h^A \bar{b}_\sigma^A b_\sigma^B + h.c.). \end{aligned} \quad (\text{D3})$$

Finally we calculate the continuum limit of L_{heis} (Eq. (63)). Let us separate it to two parts:

$$L_{\text{heis}} = L_b^0 + L_J, \quad (\text{D4})$$

$$L_b^0 = \sum_{s, \delta} \sum_{i \in s} [\bar{b}_{i\sigma} (\partial_\tau + isA_\tau(i)) b_{i\sigma} + \lambda \bar{b}_{i\sigma} b_{i\sigma}], \quad (\text{D5})$$

$$L_J = -\frac{J\Delta}{2} \sum_{\substack{i \in A \\ \delta, \sigma}} \sigma [e^{i\delta \cdot \mathbf{A}(i, i+\delta)} \bar{b}_{i\sigma} \bar{b}_{i+\delta, -\sigma} + h.c.]. \quad (\text{D6})$$

The continuum limit of L_b^0 is

$$L_b^0 \rightarrow \int \frac{d^2x}{2\Omega} \sum_{s,\sigma} [\bar{b}_\sigma^s (\partial_\tau + isA_\tau) b_\sigma^s + \lambda \bar{b}_\sigma^s b_\sigma^s]. \quad (\text{D7})$$

Next,

$$\begin{aligned} L_J &\rightarrow -\frac{J\Delta}{2} \int \frac{d^2x}{2\Omega} \sum_{\delta,\sigma} \sigma \\ &\times \left[e^{i\delta \cdot \mathbf{A}(x)} \bar{b}_\sigma^A(x - \frac{\delta}{2}) \bar{b}_{-\sigma}^B(x + \frac{\delta}{2}) + h.c. \right] \\ &\approx -\frac{J\Delta}{2} \int \frac{d^2x}{2\Omega} \sum_{\delta,\sigma} \sigma \left\{ [1 + i\delta \cdot \mathbf{A} + \frac{1}{2}(i\delta \cdot \mathbf{A})^2] \right. \\ &\times \left[(1 - \frac{\delta}{2} \cdot \nabla + \frac{1}{2}(\frac{\delta}{2} \cdot \nabla)^2) \bar{b}_\sigma^A \right. \\ &\left. \left. \cdot (1 + \frac{\delta}{2} \cdot \nabla + \frac{1}{2}(\frac{\delta}{2} \cdot \nabla)^2) \bar{b}_{-\sigma}^B \right] + h.c. \right\}. \quad (\text{D8}) \end{aligned}$$

We keep terms up to second order in a . The zeroth order terms in a are

$$L_J^0 = -4Q \int \frac{d^2x}{2\Omega} \sum_{\sigma} \sigma (\bar{b}_\sigma^A \bar{b}_{-\sigma}^B + h.c.). \quad (\text{D9})$$

Here $Q \equiv \alpha J\Delta/8$. The first order terms $L_J^1 = 0$. Using the identity

$$\begin{aligned} &\int d^2x [(\nabla^2 \bar{b}_\sigma^A) \bar{b}_{-\sigma}^B + \bar{b}_\sigma^A (\nabla^2 \bar{b}_{-\sigma}^B)] \\ &= \int d^2x [\nabla^2 (\bar{b}_\sigma^A \bar{b}_{-\sigma}^B) - 2\nabla \bar{b}_\sigma^A \cdot \nabla \bar{b}_{-\sigma}^B] \\ &= -2 \int d^2x \nabla \bar{b}_\sigma^A \cdot \nabla \bar{b}_{-\sigma}^B, \quad (\text{D10}) \end{aligned}$$

we calculate the second order terms in a :

$$\begin{aligned} L_J^2 &= -\frac{J\Delta}{2} \int \frac{d^2x}{2\Omega} \sum_{\delta,\sigma} \sigma \left\{ \left[\frac{1}{2} [(-\frac{\delta}{2} \cdot \nabla)^2 \bar{b}_\sigma^A] \bar{b}_{-\sigma}^B + \bar{b}_\sigma^A \frac{1}{2} [(\frac{\delta}{2} \cdot \nabla)^2 \bar{b}_{-\sigma}^B] + (-\frac{\delta}{2} \cdot \nabla) \bar{b}_\sigma^A (\frac{\delta}{2} \cdot \nabla) \bar{b}_{-\sigma}^B \right] \right. \\ &\quad \left. + (i\delta \cdot \mathbf{A}) [(-\frac{\delta}{2} \cdot \nabla) \bar{b}_\sigma^A] \bar{b}_{-\sigma}^B + \bar{b}_\sigma^A [(\frac{\delta}{2} \cdot \nabla) \bar{b}_{-\sigma}^B] \right\} + \frac{1}{2} (i\delta \cdot \mathbf{A})^2 \bar{b}_\sigma^A \bar{b}_{-\sigma}^B \left. \right\} + h.c. \\ &= Qa^2 \int \frac{d^2x}{2\Omega} \sum_{\sigma} \sigma \left\{ \frac{-1}{4} [(\nabla^2 \bar{b}_\sigma^A) \bar{b}_{-\sigma}^B + \bar{b}_\sigma^A (\nabla^2 \bar{b}_{-\sigma}^B)] + \frac{1}{2} \nabla \bar{b}_\sigma^A \cdot \nabla \bar{b}_{-\sigma}^B + i\mathbf{A} \cdot [(\nabla \bar{b}_\sigma^A) \bar{b}_{-\sigma}^B - \bar{b}_\sigma^A (\nabla \bar{b}_{-\sigma}^B)] + \mathbf{A}^2 \bar{b}_\sigma^A \bar{b}_{-\sigma}^B \right\} + h.c. \\ &= Qa^2 \int \frac{d^2x}{2\Omega} \sum_{\sigma} \sigma \left\{ \nabla \bar{b}_\sigma^A \cdot \nabla \bar{b}_{-\sigma}^B + i\mathbf{A} \cdot [(\nabla \bar{b}_\sigma^A) \bar{b}_{-\sigma}^B - \bar{b}_\sigma^A (\nabla \bar{b}_{-\sigma}^B)] + \mathbf{A}^2 \bar{b}_\sigma^A \bar{b}_{-\sigma}^B \right\} + h.c. \\ &= Qa^2 \int \frac{d^2x}{2\Omega} \sum_{\sigma} \sigma [(\nabla - i\mathbf{A}) \bar{b}_\sigma^A \cdot (\nabla + i\mathbf{A}) \bar{b}_{-\sigma}^B + h.c.]. \quad (\text{D11}) \end{aligned}$$

* These authors contribute equally.

† chenwq@sustech.edu.cn

‡ zcg@phy.cuhk.edu.hk

¹ J George Bednorz and K Alex Müller, "Possible high T_c superconductivity in the Ba-La-Cu-O system," *Zeitschrift für Physik B Condensed Matter* **64**, 189–193 (1986).

² F. C. Zhang and T. M. Rice, "Effective hamiltonian for the superconducting Cu oxides," *Phys. Rev. B* **37**, 3759–3761 (1988).

³ Zheng-Cheng Gu, Hong-Chen Jiang, D. N. Sheng, Hong Yao, Leon Balents, and Xiao-Gang Wen, "Time-reversal symmetry breaking superconducting ground state in the doped mott insulator on the honeycomb lattice," *Phys. Rev. B* **88**, 155112 (2013).

⁴ Zheng-Tao Xu, Zheng-Cheng Gu, and Shuo Yang, "Competing orders in the honeycomb lattice t - J model," arXiv preprint arXiv:2208.13681 (2022).

⁵ Annica M. Black-Schaffer, Wei Wu, and Karyn Le Hur, "Chiral d -wave superconductivity on the honeycomb lattice close to the mott state," *Phys. Rev. B* **90**, 054521 (2014).

⁶ Sandeep Pathak, Vijay B. Shenoy, and G. Baskaran, "Possible high-temperature superconducting state with a $d+id$ pairing sym-

metry in doped graphene," *Phys. Rev. B* **81**, 085431 (2010).

⁷ Tianxing Ma, Zhongbing Huang, Feiming Hu, and Hai-Qing Lin, "Pairing in graphene: A quantum monte carlo study," *Phys. Rev. B* **84**, 121410 (2011).

⁸ Tao Ying and Stefan Wessel, "Pairing and chiral spin density wave instabilities on the honeycomb lattice: A comparative quantum monte carlo study," *Phys. Rev. B* **97**, 075127 (2018).

⁹ Shenghan Jiang, Andrej Mesáros, and Ying Ran, "Chiral spin-density wave, spin-charge-charge liquid, and $d+id$ superconductivity in 1/4-doped correlated electronic systems on the honeycomb lattice," *Phys. Rev. X* **4**, 031040 (2014).

¹⁰ Wan-Sheng Wang, Yuan-Yuan Xiang, Qiang-Hua Wang, Fa Wang, Fan Yang, and Dung-Hai Lee, "Functional renormalization group and variational monte carlo studies of the electronic instabilities in graphene near $\frac{1}{4}$ doping," *Phys. Rev. B* **85**, 035414 (2012).

¹¹ Maximilian L. Kiesel, Christian Platt, Werner Hanke, Dmitry A. Abanin, and Ronny Thomale, "Competing many-body instabilities and unconventional superconductivity in graphene," *Phys. Rev. B* **86**, 020507 (2012).

- ¹² Rahul Nandkishore, Leonid S Levitov, and Andrey V Chubukov, “Chiral superconductivity from repulsive interactions in doped graphene,” *Nature Physics* **8**, 158–163 (2012).
- ¹³ Xiao Yan Xu, Stefan Wessel, and Zi Yang Meng, “Competing pairing channels in the doped honeycomb lattice hubbard model,” *Phys. Rev. B* **94**, 115105 (2016).
- ¹⁴ J. P. L. Faye, P. Sahebsara, and D. Sénéchal, “Chiral triplet superconductivity on the graphene lattice,” *Phys. Rev. B* **92**, 085121 (2015).
- ¹⁵ Bruno Uchoa and A. H. Castro Neto, “Superconducting states of pure and doped graphene,” *Phys. Rev. Lett.* **98**, 146801 (2007).
- ¹⁶ Zheng-Cheng Gu, Hong-Chen Jiang, and G. Baskaran, “Emergence of $p + ip$ superconductivity in two-dimensional doped dirac systems,” *Phys. Rev. B* **101**, 205147 (2020).
- ¹⁷ Philip W Anderson, “The resonating valence bond state in La_2CuO_4 and superconductivity,” *science* **235**, 1196–1198 (1987).
- ¹⁸ Patrick A. Lee, Naoto Nagaosa, and Xiao-Gang Wen, “Doping a mott insulator: Physics of high-temperature superconductivity,” *Rev. Mod. Phys.* **78**, 17–85 (2006).
- ¹⁹ Assa Auerbach, *Interacting electrons and quantum magnetism* (Springer Science & Business Media, 1998).
- ²⁰ C. Jayaprakash, H. R. Krishnamurthy, and Sanjoy Sarker, “Mean-field theory for the t - J model,” *Phys. Rev. B* **40**, 2610–2613 (1989).
- ²¹ Yosuke Nagaoka, “Ferromagnetism in a narrow, almost half-filled s band,” *Phys. Rev.* **147**, 392–405 (1966).
- ²² Daijiro Yoshioka, “Slave-fermion mean field theory of the hubbard model,” in *Strong Correlation and Superconductivity* (Springer, 1989) pp. 124–131.
- ²³ Xiao-Gang Wen, “Quantum orders and symmetric spin liquids,” *Phys. Rev. B* **65**, 165113 (2002).
- ²⁴ Fa Wang, “Schwinger boson mean field theories of spin liquid states on a honeycomb lattice: Projective symmetry group analysis and critical field theory,” *Phys. Rev. B* **82**, 024419 (2010).
- ²⁵ T. Senthil and Matthew P. A. Fisher, “ Z_2 gauge theory of electron fractionalization in strongly correlated systems,” *Phys. Rev. B* **62**, 7850–7881 (2000).
- ²⁶ T. Senthil and Matthew P. A. Fisher, “Fractionalization in the cuprates: Detecting the topological order,” *Phys. Rev. Lett.* **86**, 292–295 (2001).
- ²⁷ N. Read and Subir Sachdev, “Valence-bond and spin-peierls ground states of low-dimensional quantum antiferromagnets,” *Phys. Rev. Lett.* **62**, 1694–1697 (1989).
- ²⁸ Naoto Nagaosa, *Quantum field theory in condensed matter physics* (Springer Science & Business Media, 1999).
- ²⁹ Meng Cheng, Kai Sun, Victor Galitski, and S. Das Sarma, “Stable topological superconductivity in a family of two-dimensional fermion models,” *Phys. Rev. B* **81**, 024504 (2010).
- ³⁰ Ching-Kai Chiu, Jeffrey C. Y. Teo, Andreas P. Schnyder, and Shinsei Ryu, “Classification of topological quantum matter with symmetries,” *Rev. Mod. Phys.* **88**, 035005 (2016).
- ³¹ Masatoshi Sato and Yoichi Ando, “Topological superconductors: a review,” *Reports on Progress in Physics* **80**, 076501 (2017).
- ³² N. B. Kopnin and M. M. Salomaa, “Mutual friction in superfluid ^3He : Effects of bound states in the vortex core,” *Phys. Rev. B* **44**, 9667–9677 (1991).
- ³³ GE Volovik, “Fermion zero modes on vortices in chiral superconductors,” *Journal of Experimental and Theoretical Physics Letters* **70**, 609–614 (1999).
- ³⁴ N. Read and Dmitry Green, “Paired states of fermions in two dimensions with breaking of parity and time-reversal symmetries and the fractional quantum hall effect,” *Phys. Rev. B* **61**, 10267–10297 (2000).
- ³⁵ A. Möller, U. Löw, T. Taetz, M. Kriener, G. André, F. Damay, O. Heyer, M. Braden, and J. A. Mydosh, “Structural domain and finite-size effects of the antiferromagnetic $S = 1/2$ honeycomb lattice in $\text{InCu}_{2/3}\text{V}_{1/3}\text{O}_3$,” *Phys. Rev. B* **78**, 024420 (2008).
- ³⁶ Zheng-Cheng Gu, “Efficient simulation of grassmann tensor product states,” *Phys. Rev. B* **88**, 115139 (2013).
- ³⁷ Zheng-Cheng Gu, Frank Verstraete, and Xiao-Gang Wen, “Grassmann tensor network states and its renormalization for strongly correlated fermionic and bosonic states,” arXiv preprint arXiv:1004.2563 (2010).
- ³⁸ Henrik Bruus and Karsten Flensberg, *Many-body quantum theory in condensed matter physics: an introduction* (OUP Oxford, 2004).